Update of CPUE abundance index using GAM for southern bluefin tuna in CCSBT (GAM22) up to the 2024 data

CCSBT のミナミマグロについての GAM を用いた CPUE 資源豊度指数 (GAM22) の 2024 年データまでの更新

Tomoyuki ITOH and Norio TAKAHASHI

伊藤智幸・高橋紀夫

Fisheries Resources Institute, Japan Fisheries Research Agency 水産研究·教育機構 水産資源研究所

要約

2022年 ESC27では、GAM を用いた 2 段階のデルタログノーマルアプローチで CPUE を標準化して面積重みづけする、新たなミナミマグロの CPUE 資源量指数の作成方法に合意した。合意された方法に従った CPUE 資源量指数(GAM22 と称す)の作成を、2024年までの漁獲データに対して実施した。本文書ではベースケースの結果と、様々な感度分析を行った結果を示す。得られた指数値では 2024年に 2023年よりも増加し、1969年からのシリーズでの最高値に達した。モデル選択、レトロスペクティブ解析、対象年齢の変更を含む様々な感度分析に対して資源量指数は頑健であった。操業の無い時空間は年々増加しており、それらに対する予測 CPUE が高い値を示す場合があった。

Summary

At ESC27 in 2022, the new calculation for the abundance index of southern bluefin tuna, which was standardized via a generalized additive model in the two-step delta log-normal approach with area weighting, was agreed. The CPUE abundance index, referred to as *GAM22*, was updated for fishery data up to 2024 according to the agreed methodology. This document presents the base case results as well as the results of various sensitivity tests. The index value increased in 2024 from 2023 and reached the highest value since 1969. The abundance index was robust to a variety of sensitivity analyses, including model selection, retrospective analysis, and age range changes. The amount of time and space without fishing operations has been increasing, and the predicted CPUEs for these time and space were sometimes high.

1. Introduction

Stock assessment and stock management through the Management Procedure (MP) of southern bluefin tuna (*Thunnus maccoyii*; SBT) in CCSBT have historically been strongly relied on the abundance index obtained from the CPUE (number of fish / 1000 hooks) of the Japanese commercial longline fishery. In the old days, Nishida and Tsuji (1998) developed a model to calculate the abundance index by the generalized linear model (GLM). Since 2007, alternative abundance index was developed which called the core vessel CPUE standardized by GLM in response to the shrinking operating area in time and space and the problem of target fish species (ESC12 report, Itoh et al. 2008). The CPUE abundance index had been used as one of the main abundance indices in the two MPs of the Bali procedure used for the TAC calculation from 2012 to 2020 and the Cape Town Procedure (CTP) used for the TAC calculation since 2021.

It was recognized that the 2018 value of the CPUE abundance index by the core vessel CPUE was anomalously high in ESC24 held in 2019 (ESC24 Report). This prompted further investigation, which subsequently identified that this estimate was generated due to a prediction bias in the GLM standardization method being used, which generated anomalously high estimates for cells with no fishing effort. At ESC26 in 2021, it was agreed that a new CPUE abundance index should be prepared by May 2022 to assess its impact on MP (ESC26 Report). Through the collaboration work between Japanese scientists and the consultant hired by CCSBT, as well as the discussion and suggestion of the CPUE working group, a new abundance index using CPUE standardized by the generalized additive model (GAM) was developed and agreed at ESC27 in 2022 (OMMP12 and ESC27 Reports). Here, we refer to the abundance index as *GAM22*, because it was agreed in 2022.

This document presents the CPUE results obtained by updating the data to 2024 using the agreed GAM methodology not only for the base case but also for the various sensitivity analyses (Itoh and Takahashi 2022, 2023a, 2024). We have also included a detailed review of predicted value from model for the time and space with no effort (Itoh and Takahashi 2023b).

2. Materials and Methods

2-1. Dataset used

The dataset was extracted from logbook data for the Japanese longline fishery, which include the period from 1969 to the latest year (currently 2024). Following procedures for the conventional SBT CPUE abundance index, records in statistical Areas between 4 and 9 and from April to September were selected. From the logbooks, year, month, latitude (in 1 degree), longitude (in 1 degree), vessel ID (available from 1979), number of hooks used, number of fish caught of SBT, bigeye tuna (*T. obesus*, BET), yellowfin tuna (*T. albacares*, YFT), albacore (*T. alalunga*, ALB) and swordfish (*Xiphias gladius*, SWO) data were used. In the development work in 2022, the number of hooks between floats (HBF; available since 1975) and other fish species (several species of marlines, and butterfly kingfish (*Gasterochisma melampus*; available since 1994)) were examined and we decided not to use them so that these items were not included in the work this year.

From the size data of the CCSBT database, the age composition of Japanese commercial catch was calculated and converted into the number of fish caught age-4 and older (age-4 plus). The age composition information was first applied to the fork length composition of 50 or more individuals measured in the same month, 5 degrees longitude, and 5 degrees latitude. At this stage, 97% of the number of SBT caught was incorporated and the ratio of age-4 plus was calculated. For records of the conditions for 50 or more individuals were not met the time and space were gradually expanded to correspond to fork length composition, such as the same month - longitude 15 degrees - latitude 5 degrees, the same month -

longitude 15 degrees - latitude 15 degrees, the same quarter - longitude 15 degrees - latitude 5 degrees, the same quarter - Statistical Area (CCSBT Statistical Area), and the same year - Statistical Area, and the same year. The fork length was converted to age by the age-length relationship used by CCSBT. Sensitivity analysis was conducted for age-5 plus and all ages.

The following records were eliminated: hooks 500 or less, hooks 4500 or more, CPUE 200 or higher. As a result of the examination, with the agreement in the CPUE working group discussion in 2022, the record of 50S (50S to 54S), which had a small number of data, were also eliminated.

2-2. Cluster analysis

A cluster analysis was performed to consider the target species of the fishing operations. The *clust_PCA_run* function of the R package *cpue.rfmo* was used. Cluster analysis was performed using the number of fish caught of five species, SBT, BET, YFT, ALB and SWO as data.

2-3. Standardization by GAM

Standardization by the generalized additive model (GAM) was carried out by using the delta log-normal approach. A software for statistical computing and graphics, R (R Core Team 2025) was used for analysis. The *bum* function, which is suitable for large volumes of data, in the mgcv package was used. Based on the results of the study by the consultant (Dr. Hoyle), a binomial submodel (hereinafter referred to as BSM) and a positive catch submodel (hereinafter referred to as PCSM) were used, and gamma = 2, binomial distribution and gauss distribution were used respectively (Hoyle 2022). For the smoother, s (spline) was used for the offset term (hook logarithmic value), and ti (tensor product suitable when there was an interaction with the main effect) was used for the others. cs (cubic regression spline with shrinkage) was used for the basis function (bs) of ti. Gamma is a coefficient multiplied by EDF (described later) and promotes smoothing with values set to >1 (= 1.5 is common).

```
Binomial submodel

cpue > 0 ~ yf +ti(month) + ti(lon) + ti(lat) +

ti(lon, lat) + ti(month, lat) + ti(lon, month) + ti(year, lat) + ti(year, lon) + ti(year, month) +

cl + s(log(hook))

Positive catch submodel

log(cpue) ~ yf +ti(month) + ti(lon) + ti(lat) +

ti(lon, lat) + ti(month, lat) + ti(lon, month) + ti(year, lat) + ti(year, lon) + ti(year, month) +

ti(lat, month, year) + ti(lat, lon, month) + ti(lat, lon, year) + ti(year, lon, month) +

cl + s(log(hook))

where,

yf: Year of fishing. In factor.

year: Year. In number

month: Month. In number

lat: Latitude in 5 degree. In number. Represented by the middle (e.g. -47.5 from 45.0S to 49.9S)

lon: Longitude in 5 degrees. In number. Represented by the middle (e.g. 32.5 for 30.0E to 34.9E).
```

Convert to 360 degree while >240 was converted by -360 so that lon ranged from -22.5 to 187.5 continuously.

cl: Cluster. In factor. 1, 2, 3, and 4.

hook: Number of hooks used. In number.

R code actually used is as follows.

Binomial submodel

```
modA2 <- cpue > 0 \sim yf +
                                       k=kA.month11,bs="cs")+
                       ti(month,
                       ti(lon,
                                       k=kA.lon11,bs="cs")+
                       ti(lat,
                                       k=kA.lat11,bs="cs")+
                       ti(lon, lat,
                                       k=c(kA.lon21, kA.lat21), bs="cs")+
                       ti(month, lat,
                                       k=c(kA.month22,kA.lat22), bs="cs")+
                       ti(lon, month, k=c(kA.lon23, kA.month23), bs="cs")+
                                       k=c(kA.year24, kA.lat24), bs="cs")+
                       ti(year, lat,
                       ti(year, lon,
                                       k=c(kA.year25, kA.lon25), bs="cs")+
                       ti(year, month, k=c(kA.year26, kA.month26), bs="cs")+
                       cl+
```

mgcv::bam(modA2, data =data, gamma = 2, method = 'fREML', family = binomial, discrete=F)

s(log(hook))

Positive catch submodel

```
modB3 < -log(cpue) \sim yf +
                      ti(month,
                                              k=kB.month11,bs="cs")+
                      ti(lon.
                                              k=kB.lon11,bs="cs")+
                      ti(lat,
                                              k=kB.lat11,bs="cs")+
                      ti(lon, lat,
                                              k=c(kB.lon21, kB.lat21), bs="cs")+
                                              k=c(kB.month22,kB.lat22), bs="cs")+
                      ti(month,lat,
                      ti(lon, month,
                                              k=c(kB.lon23, kB.month23), bs="cs")+
                                              k=c(kB.year24, kB.lat24), bs="cs")+
                      ti(year, lat,
                      ti(year, lon,
                                              k=c(kB.year25, kB.lon25), bs="cs")+
                      ti(year, month,
                                              k=c(kB.year26, kB.month26), bs="cs")+
                      ti(lat, month, year,
                                              k=c(kB.lat31, kB.month31, kB.year31), bs="cs")+
                      ti(lat, lon, month,
                                              k=c(kB.lat32, kB.lon32, kB.month32), bs="cs")+
                      ti(lat, lon, year,
                                              k=c(kB.lat33, kB.lon33, kB.year33), bs="cs")+
                      ti(year, lon, month,
                                              k=c(kB.year34, kB.lon34, kB.month34), bs="cs")+
                      cl+
                      s(log(hook))
```

mgcv::bam(modB3, data = data.positive, gamma = 2, method = "fREML", discrete=F)

The larger the k value (basis dimension for smoothing flexibility) of the interaction, the better, but the longer the calculation time (Wood, help of *choose.k* in mgcv). The effective degrees of freedom for a model term (EDF) value is calculated by the *k.check* function in mgcv package, and if EDF was close to k' (the maximum possible EDF for the term), "and" the p-value of k-index is < 0.05, a larger k value was set. The k values were determined by trial and error. Since the k value of the interaction is treated as the value of 2 multiplications (3 multiplications for 3 interactions), it is not necessary to set them separately, however, for the purpose of organizing the work, the k value of each variable in the interaction was set to the same value (i.e. k for year = 20 was used for all interaction terms which include year).

For the diagnosis of the GAM result, the fit was confirmed by the plot diagram (QQ plot, residual distribution) by the *gam.check* function of the mgcv package. AIC was calculated. The distribution of the residuals for each variable was examined. It was examined whether the predicted values were consistent with our knowledge of distribution of SBT and plausible trend of SBT stock abundance. We made a comprehensive judgment by looking at this information as well as AIC.

Calculation is performed by a desktop PC (CPU = Intel (R) Core (TM) i9-10900T CPU @ 1.90GHz and 1.90 GHz, RAM = 64.0GB, 64 bit, Windows 10 Pro). The software R (R4.4.1) was used to make the dataset. Microsoft R Open 4.0.2 was used to calculate GAM.

2-4. Calculation of abundance index

After creating data with all combinations of year / month / latitude / longitude (using R's *expand.grid* function), we made a dummy data set limited to the month / latitude / longitude where the fishing was operated in the past. The predicted value was calculated for each submodel for the dummy data set, and the product of estimates from the two submodels (BSM and PCSM) was calculated. Since the expected value is biased when the log-normal distribution is restored, the predicted value was corrected by adding mean squared error (MSE) / 2 in the case of the positive catch submodel.

Furthermore, the area weighting coefficient was calculated in consideration of the fact that the distance of 1 degree of longitude differs depending on the latitude and the number of 1 degree squares that SBT have been caught in the past within the 5 degree x 5 degree squares. The abundance index can be calculated by the following formula.

 Σ (predicted value of binomial submodel of dummy data set \times predicted value of positive catch submodel of dummy data set \times Area weighting coefficient) / Overall average value.

2-5. Sensitivity analysis

Various sensitivity analyses were performed along the way in selecting the datasets and methods. The same sets of sensitivity analyses performed at the final stage in 2022 were repeated in 2023 and 2024. We omitted some of the analyses where no substantial difference was observed.

Model selection: In some cases, estimation did not converge, and in some cases, even if the AIC was low, the abundance index behaved significantly differently from the others, so a simple selection by AIC seemed inappropriate. For the binomial submodel, we tried the case where all the interactions were removed from the base case, the case where the two-way interaction was removed one by one, and the case where all the interactions were removed from the base case, the case where the two-way interaction was removed one by one, and the case where the three-way interaction was removed one by one, and the case where the three-way interaction was removed one by one.

Retrospective analysis: Excludes data from the last year up to the past 10 years. Mohn's rho was

calculated as an index of retrospective bias (Hurtado-Ferro et al. 2015).

Selection of k: Effect when k was increased by one step.

Effect of changing age: Age-4 plus used in the base case, but limited to age-5 plus, or all ages were tried.

2-6. Abundance indices by historical models

We compared the newly created abundance index (GAM22) with other models used in CCSBT including the core vessel index by the conventional GLM (GLM core).

The GLM model is as follows (Itoh and Takahashi 2022):

```
log(CPUE+0.2) = Intercept + Year + Month + Area + Lat5 + BET_CPUE + YFT_CPUE + (Month*Area) + (Year*Lat5) + (Year*Area) + Error,
```

where year, month, area, lat5 were treated as factors. A Gaussian distribution was used for the error term. *glm* function of R was used. Note that the whole dataset was applied instead of restricted to the core vessel data. A Gaussian distribution was used for the error term. W0.8, which weighed indices of 80% Constant and 20 % Variable square hypotheses, was used for the index.

2-7. Analysis of predicted value

To each record of the dummy data set, the number of operations in actual fishery data was attached. Predicted values were calculated for each combination of variables by GLM (GLM_core) and GAM (GAM22), respectively (both area weighted). The dataset was classified into four groups based on the number of operations actually given. Group 0 has 0 operations, Group 1 has 1 to less than 5 operations, Group 2 has 5 to less than 10 operations, and Group 3 has 10 or more operations.

A higher CPUE is expected in a space-time stratum with a higher number of operations. This is because there would be a high probability that a vessel does not stay in a space-time stratum with a low CPUE, and it is expected that operations are not conducted in a space-time stratum with a low CPUE through the accumulation of historical knowledge. Boxplot is used for visualization.

3. Results

3-1. Dataset used

Data from 1969 to 2024 amounted to 803,697 records. Of these, 710,827 records included a catch of SBT age-4 plus, accounting for 88% of the total. A very high positive catch rate is characteristic of this dataset. By year, the positive catch rate dropped to about 60% in the mid-1990s and around 2010, but otherwise remained above 80% (Fig. 1). The percentage was high in 2024 as well as 2023, and few low values were observed in the aggregated month and 5-degree data (Fig. 1, center panel). The nominal CPUE of the positive catch dataset is high in the 1970s, low in the 1980s to 2000s, and high after 2010. The nominal CPUE in 2024 was the highest in the past 40 years.

Similar figures are shown for other variables, including month, longitude, latitude, latitude and longitude maps (Fig. 2 and Fig. 3). There is no strong tendency for the month and longitude. For latitude, positive rate and CPUE in the positive catch data was low at 30S, high up to 35S (CPUE) or 40S (positive rate), and 45S was similar to 40S. Data of 30S exists only in the Pacific Ocean (Area 4 and Area 5).

3-2. Cluster analysis

The data were divided into four cluster groups. Relevant figures are shown in Fig. 4 to Fig. 8. Since

the eigenvalues are greatly reduced to 2 groups and the decrease to 4 groups is not so large, it may be appropriate to divide them into 2 groups. However, in the analysis of the data up to 2020, there was a problem that the BSM of GAM did not converge when divided into two groups (the data up to 2021 converged in a short time). Therefore, we decided to analyze in 4 groups. Note that the case of 2 groups was carried out by sensitivity analysis in previous years.

The fish species included five species: SBT, BET, YFT, ALB and SWO. At the stage of trial and error in the 2022 work, we also tried 3 species (SBT, BET and YFT) and obtained similar results as 5 species. But 3 species are few and cover all species that can be the main target of operation, it was decided by the CPUE working group to have 5 species (Itoh and Takahashi 2022).

The latitudes of the four clusters differed (Fig. 7), however, there were no noticeable trends in year, month, longitude, number of hooks used, or hooks between floats (HBF). It was probable that HBF had a narrow range in the dataset and did not make a difference because it contained few data of deep longline targeting on BET. Such an effect may have been seen in the waters north of the Area 4-9. The main catch in the first cluster which is located southernmost was SBT. SBT and ALB were caught in the second cluster. The third cluster was a mixture of five species and the fourth cluster was a mixture of SBT, ALB.

3-3. Standardization by GAM

For the binomial submodel, the model including all main effects and two-way interaction terms was selected mainly from AIC in the 2022 work. There was a problem that the run did not converge when the three-way interaction term was included. For the positive catch submodel, the model including the main effect and all the two-way and three-way interaction terms was selected mainly from AIC. It was agreed in the ESC in 2022 that these models were used for the base case.

The k value was examined independently for each submodel. The same sets of k used in the 2022 work were utilized (Table 1). Table 2 shows relevant statistics including the EDF value for k and the p value for k-index. The ti (lat) in the positive catch submodel has close EDF value to k' (2.97 to 3) and p-value 0.03 is below 5% can be a problem, however, k value for latitude has already reached the maximum.

The diagnosis results are shown in Table 3, Fig. 9, and Fig. 10. The binomial submodel explained 73.8% deviance, and the positive catch submodel explained 49.5%. For BSM, the QQ plot is generally good, although some parts do not fit at both ends. The residual histogram has a single peak and is skewed to near 0 residual. For PCSM, the QQ plot is generally good, and the residual has a single peak. In the plot of the fit value and the response variable, there is a roughly upward-sloping relationship. Both are judged to be not bad fit.

The residuals were further examined. Plots were made for year, month, latitude, and longitude (Figs. 11 and 12). Note that these figures are not from *gamVis*, which uses simulation. There was too much data and *gamVis* caused a memory over and so we couldn't get any results. These are simple box plots of residuals. For BSM, the median residuals were positively biased in 2004-2007 in the year. There was a slight positive bias for month. At latitude, the negative bias was large at 30S, a slight positive bias was seen at 35S, and the bias was small at 40S and 45S. At the western end of the longitude, there was a large negative bias.

For PCSM, the bias was small by year and month. At latitude, the range was large at 30S. The bias of the longitude was small, but a negative bias was seen only at the eastern end. When made into a map, the area with zero residuals was greatly expanded in both submodels (Fig. 13). In some places, large residuals may occur in the peripheral waters. It has been confirmed in the 2022 work that the data in the area where these large residuals are seen has negligible impact on the abundance index.

Box plots of predicted values for variables (year, month, latitude, longitude, latitude x longitude) in the dummy dataset are shown (Fig. 14, Fig. 15, Fig. 16, Fig. 17 and Fig. 18). No inconsistency was found in

comparison with the current knowledge of the distribution of SBT and changes in the abundance. The high predicted values in the southeastern waters of Australia (35S, 140E) are interesting (Fig. 18). Currently, there is no fishing operation in this area, but it was confirmed in the 2022 work that the fishing was operated in this area in the 1970s and 1980s.

3-4. Calculation of abundance index GAM22

The predicted value of the dummy data set was weighted by the area factor and normalized by the average value to obtain the abundance index as GAM22. To see the effect of area weighting, we compared it with a simple unweighted average (Fig. 19). As a result, it was found that they are similar to each other, and the influence of weighting is small. Since this method includes the interaction of years in the model, it is no longer necessary to obtain the conventional Constant / Variable square hypothesis and its intermediate index (see Hoyle (2022) for details).

Figure 20 shows the obtained abundance index of GAM22. The values are shown in Table 4. It increased in many years from 2006 to 2024. In 2024, it is the highest value since 1969.

3-5. Sensitivity analysis

Model selection

For BSM, a model (modA2) containing all two-way interactions was selected as the base case in the 2022 work. Its AIC was lower than any other model with one term removed from modA2 (Table 5). On the contrary, in the model to which one three-way interaction term was added (e.g. modA2.p11), the AIC was low, but there was a problem that it did not converge sometimes. The difference on the abundance index was small in the models (Fig. 21 and Fig. 22). Therefore, it is considered appropriate to use modA2 as the base case this year again.

For PCSM, a model (modB3) containing all the two-way and three-way interaction terms was selected as the base case in the 2022 work. Its AIC was lower than any other model with one term removed from modB3 (Table 6). The modB3 was used as the base case this year again. The difference between the models in the abundance index is small (Fig. 23 and Fig. 24). Relatively large differences were seen in modB3.no9 and mdB3.no10 which excluding ti(year, lon) and ti(year, month), respectively.

Retrospective analysis

Figure 25 shows the results of retrospective analysis of the base case model. Figure 26 shows the results by each submodel. Differences were small in previous years. Mohn's rho was 0.11, less than the +0.20 that indicates caution (Hurtado-Ferro et al. 2015).

Selection of k

For BSM, we examined the effect of adding +1 to k of the month, +5 to k of the year, and +5 to k of the longitude. The latitude has already reached the maximum value (k = 4). For PCSM, we examined the effect of increasing the year k by +5 and the longitude k by +5. The month and latitude are already at their maximum.

As a result, there was very little effect on BSM (Fig. 27 and Fig. 28), however, there is some change when kA.year25 (ti(year, lon)) was changed from 10 to 15. It is suggested that k was large enough for most cases. For PCSM, there was a noticeable change when kB.year34 (ti (year, lon, month)) or kB.year33 (ti (lat, lon, year)) was changed from 20 to 25 (Fig. 29, Fig. 30). It might be better to consider increasing these k-values associated with year in future.

Effect of changing age range

The results are shown for the base case of age-4 plus, limited to age-5 plus (Fig. 31), and for all ages (Fig. 32). At the age-5 plus, the overall trajectory was similar to the base case up to 2023, but significantly lower in 2024 values. For all ages, the values for 1990-1994 and 2017-2023 were slightly higher, but that in 2024 was much higher.

This sensitivity analysis is related to not only cohort strength but also release and discard. When fish is released and discarded from longline vessels, it is often a small fish, age-3 or age-4. The proportion of released fish will depend on the vessel's IQ utilization strategy. If the proportion of released fish changes in a certain year in the future, the effect can be examined by calculating the abundance index for those ages other than 4 and comparing it with the abundance index for those age-4 plus. The proportion of the number of fish released from Japanese longliners has been monitored and calculated as 3.8% of total catch of age 4 plus in average (Itoh 2025).

3-7. Analysis of predicted value

Figure 33 shows the proportion of each group of the number of operations conducted in the dummy dataset by year. The value for 2024 is provisional and may increase as data input work progresses. The proportion has decreased since 1969, indicating a decrease in the proportion of time-space in which operations took place. While it was stable in the 1980s, the decline has continued since 1990.

Figure 34 shows the predicted CPUE values by group in data all years combined, by GLM_core and GAM22. As expected, the time and space with higher operation numbers had higher CPUE. The same figure is shown in Fig. 35, including the boxplot outlier. It is apparent that there are anomalously high predicted outliers in GLM_core and fewer in GAM22.

A similar figure is shown in Fig. 36 by year. From 1969 to 2007, the box part is wide and the CPUE increases according to the increase in the number of operations. From around 2008, outliers became higher as the box area was compressed in the figure. From 2018, the outliers were particularly high in GLM_core, and it was significantly different from the figure by GAM22. Fig. 37 shows the change in outliers over time in the space-time without operations. Extremely large outliers are observed in 2018 and 2019 in GLM_core and lesser extent in 2022, 2023 and 2024 in GAM22. These came from Area 8 between June to September for GLM_core (Table 7) and Area 4 between July and September and Area 7 in April for GAM22 (Table 8). Outliers in GAM22 were not extremely high.

4. Discussion

The 2024 fishing data was added to the dataset. The method using GAM agreed at the 2022 ESC was able to obtain a convergent solution without changing the settings such as the k parameter to the updated dataset. The distribution of the residuals for each variable and the overall fitting of the residuals in the base case were the same as in the previous work, and no problems were observed. The results of the sensitivity analysis were similar to those of the 2022, 2023 and 2024 works.

High CPUE was predicted in 2022, 2023 and 2024 where fishing was not conducted. While this is not as significant an issue as the 2018 GLM_core, the predictions for the non-fished space-time will require careful interpretation and future monitoring.

5. References

- CCSBT (2007) Report of the Twelfth Meeting of the Scientific Committee. 10 14 September 2007. Hobart, Australia. 80pp.
- CCSBT (2019) Report of the Twenty Fourth Meeting of the Scientific Committee. 7 September 2019. Cape Town, South Africa. 121pp.
- CCSBT (2021) Report of the Twenty Sixth Meeting of the Scientific Committee. 31 August 2021. Online. 93pp.
- CCSBT (2022a) Report of the Twelfth Operating Model and Management Procedure Technical Meeting. 20-24 June 2022. Hobart, Australia and Online. 33pp.
- CCSBT (2022b) Report of the Twenty Seventh Meeting of the Scientific Committee. 29 August-5 September 2022. Online. 114pp.
- Hoyle, S. (2022) Validating CPUE model improvements for the primary index of southern bluefin tuna abundance. CCSBT-OMMP/2206/04.
- Hurtado-Ferro, F., Szuwalski, C.S., Valero, J.L., Anderson, S.C., Cunningham, C.J., Johnson, K.F., Licandeo, R., McGilliard, C.R., Monnahan, C.C., Muradian, M.L., Ono, K., Vert-Pre, K.A., Whitten, A.R., Punt, A.E., (2015) Looking in the rear-view mirror: bias and retrospective patterns in integrated, age-structured stock assessment models. ICES J. Mar. Sci. 99–110.
- Itoh, T., E. Lawrence, and J. G. Pope (2008) The development of new agreed CPUE series for use in future MP work. CCSBT-ESC/0809/09.
- Itoh, T. and N. Takahashi (2022) Development of the new CPUE abundance index using GAM for southern bluefin tuna in CCSBT. CCSBT-OMMP/2206/08.
- Itoh, T. and N. Takahashi (2023a) Update of CPUE abundance index using GAM for southern bluefin tuna in CCSBT up to the 2022 data. CCSBT-OMMP/2306/05
- Itoh, T. and N. Takahashi (2023b) Further examination of CPUE abundance index using GAM for southern bluefin tuna based on predicted values, CCSBT-OMMP/2306/09.
- Itoh, T. and N. Takahashi (2024) Update of CPUE abundance index using GAM for southern bluefin tuna in CCSBT up to the 2023 data. CCSBT-ESC/2409/21.
- Itoh, T. (2025) Change in operation pattern of Japanese southern bluefin tuna longliners in the 2024 fishing season. CCSBT-OMMP/2507/05.
- Nishida T. and S. Tsuji (1998) Estimation of abundance indices of southern bluefin tuna (*Thunnus maccoyii*) based on the coarse scale Japanese longline fisheries data (1969-97). CCSBT/SC/9807/13.
- R Core Team (2025) R: A Language and Environment for Statistical Computing. R Foundation for Statistical Computing, Vienna, Austria. https://www.R-project.org/>.

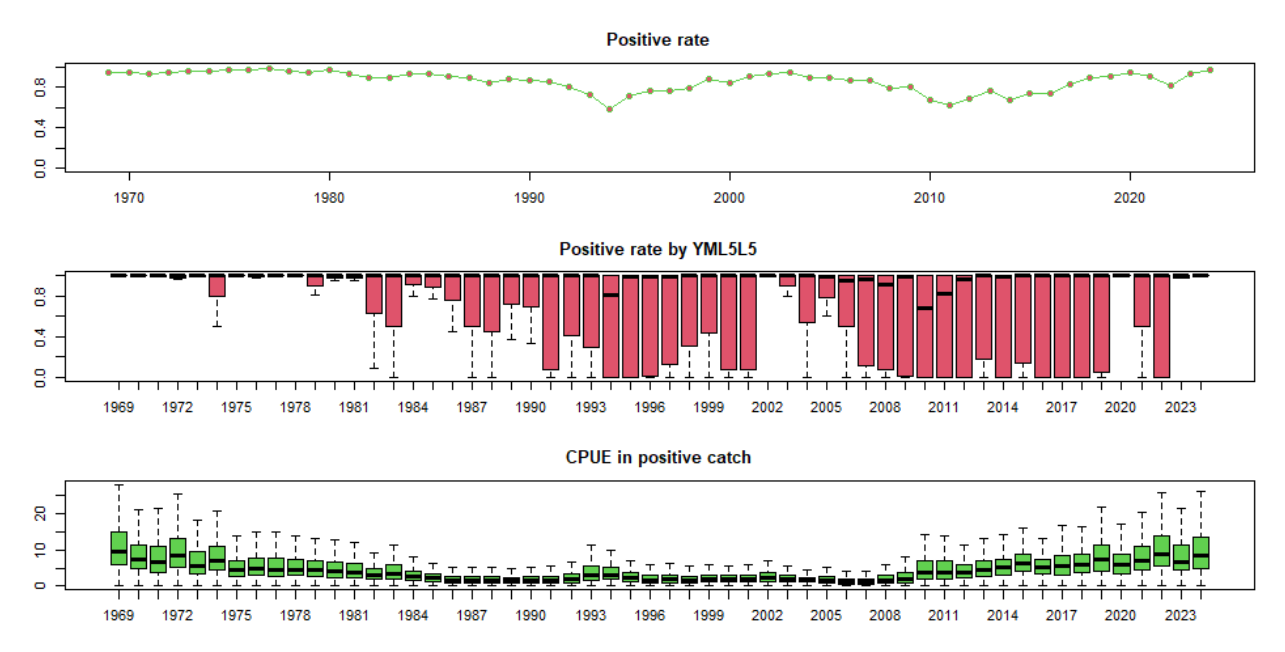


Fig. 1. Nominal value of positive catch rate and CPUE by year.

Upper panel is the positive rate which is the total number of positive catch operations / the total number of all records. Middle panels is boxplot based on the positive catch rate by year, month, 5 degree latitude and 5 degree longitude. Lower panel is CPUE in positive catch records.

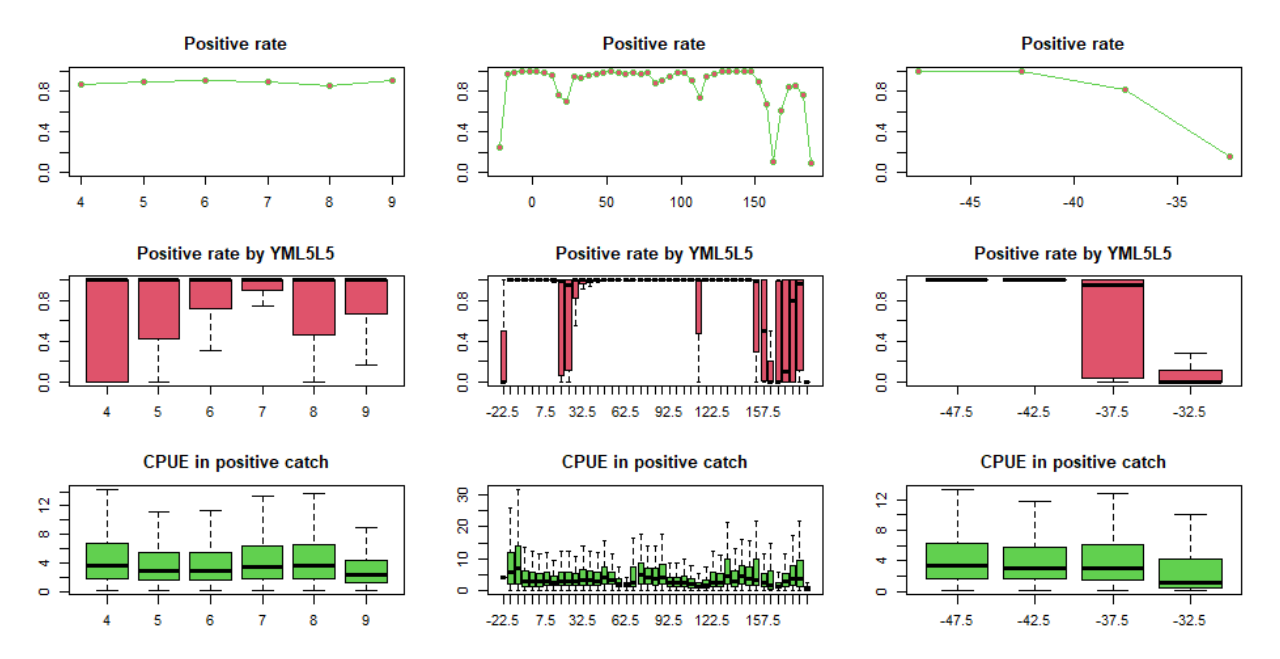


Fig. 2. Nominal value of positive catch rate and CPUE by month, longitude and latitude.

Upper panels are the positive rate which is the total number of positive catch operations / the total number of all records. Middle panels are boxplot based on the positive catch rate by year, month, 5 degree latitude and 5 degree longitude. Lower panels are CPUE in positive catch records.

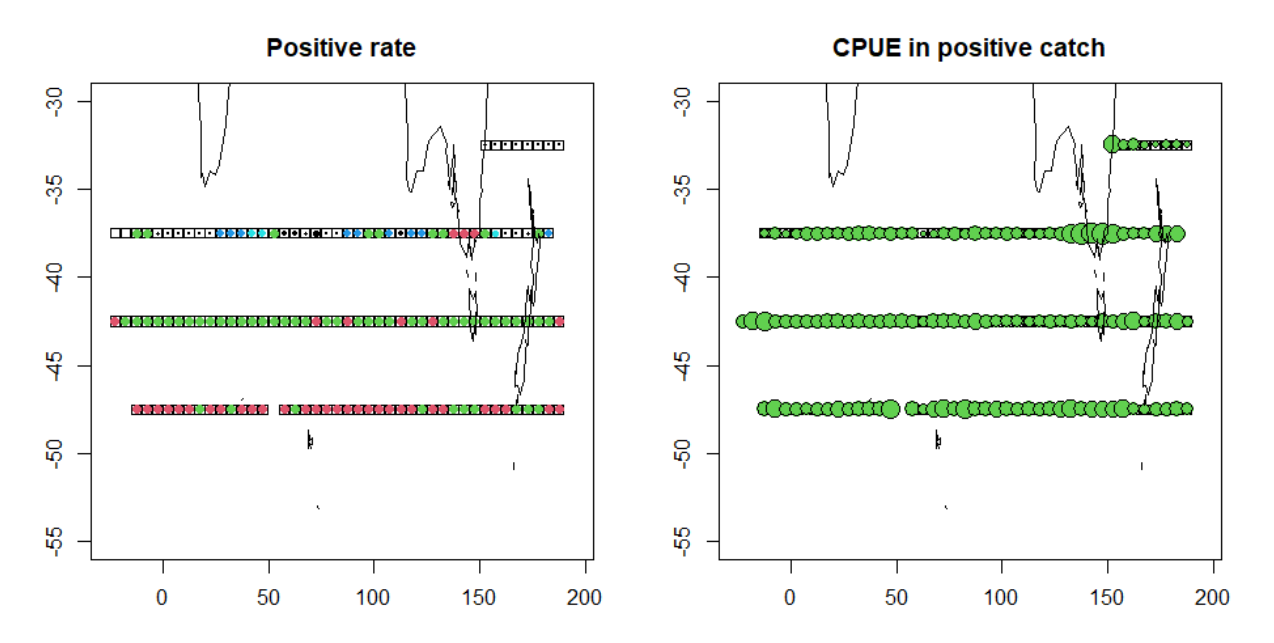


Fig. 3. Nominal value of positive catch rate and CPUE in map.

Left panel is the positive rate. Right panel is CPUE in positive catch records. Red is the higher value, followed by green, blue and white in the positive catch rate panel.

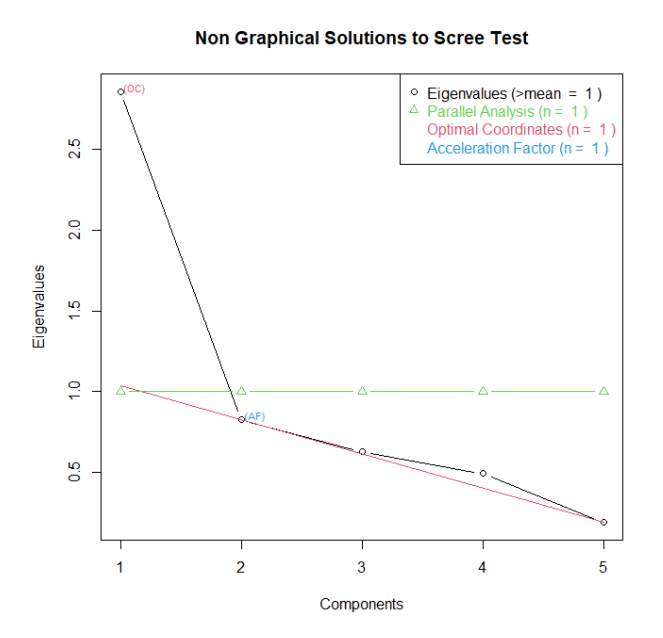
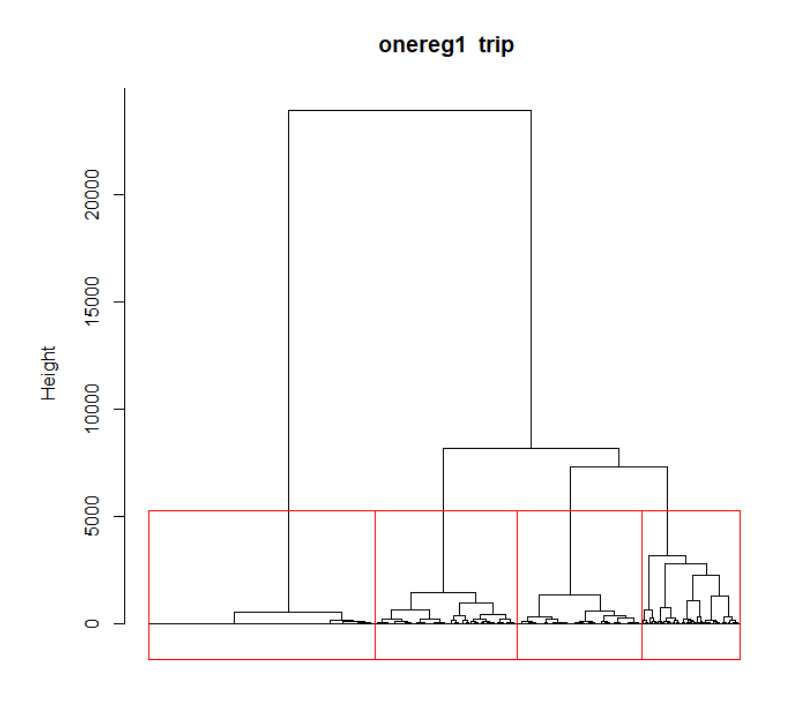


Fig. 4. Eigen values for the number of components in cluster analysis.



dtrp fastcluster::hclust (*, "ward.D")

Fig. 5. Dendrogram of the cluster analysis.

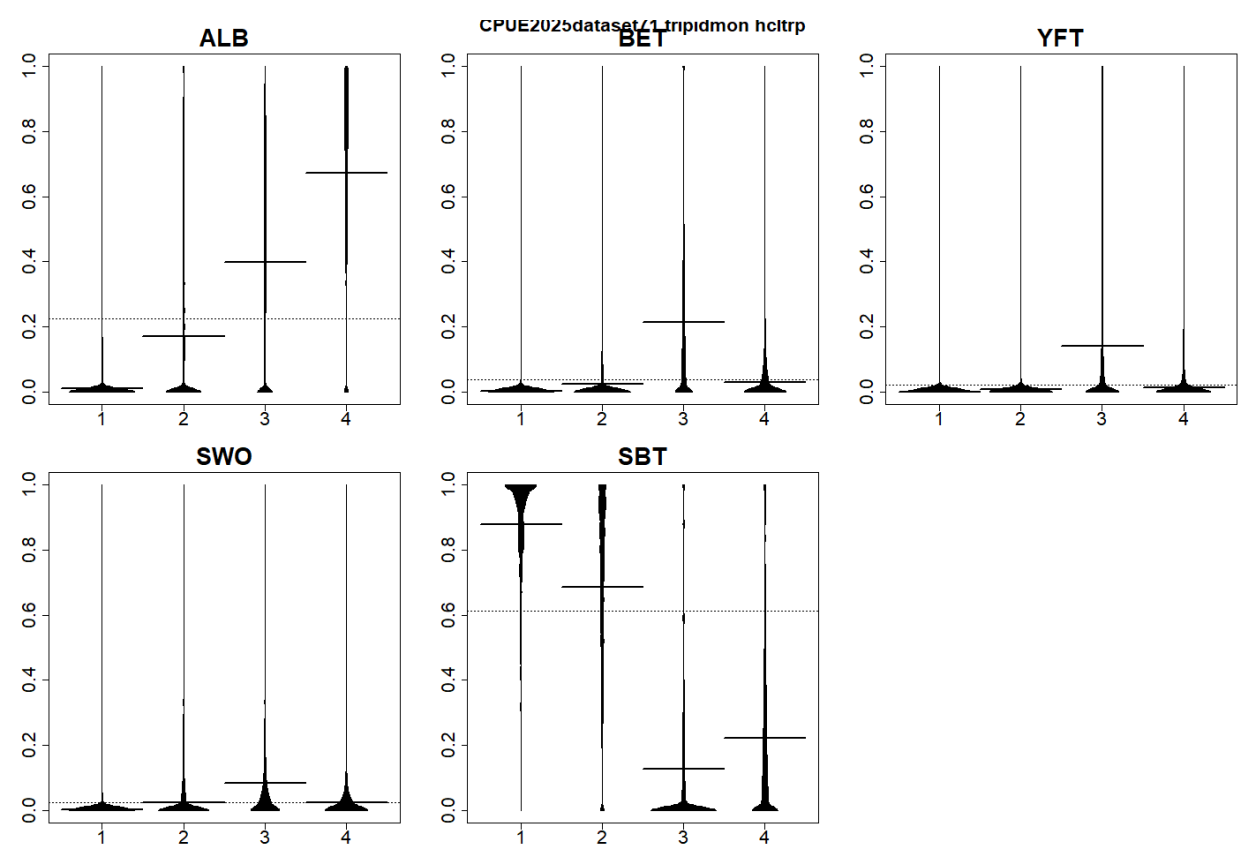


Fig. 6. Occurrence by species in each group in cluster analysis.

ALB is albacore, BET is bigeye tuna, YFT is yellowfin tuna, SWO is swordfish and SBT is southern bluefin tuna.

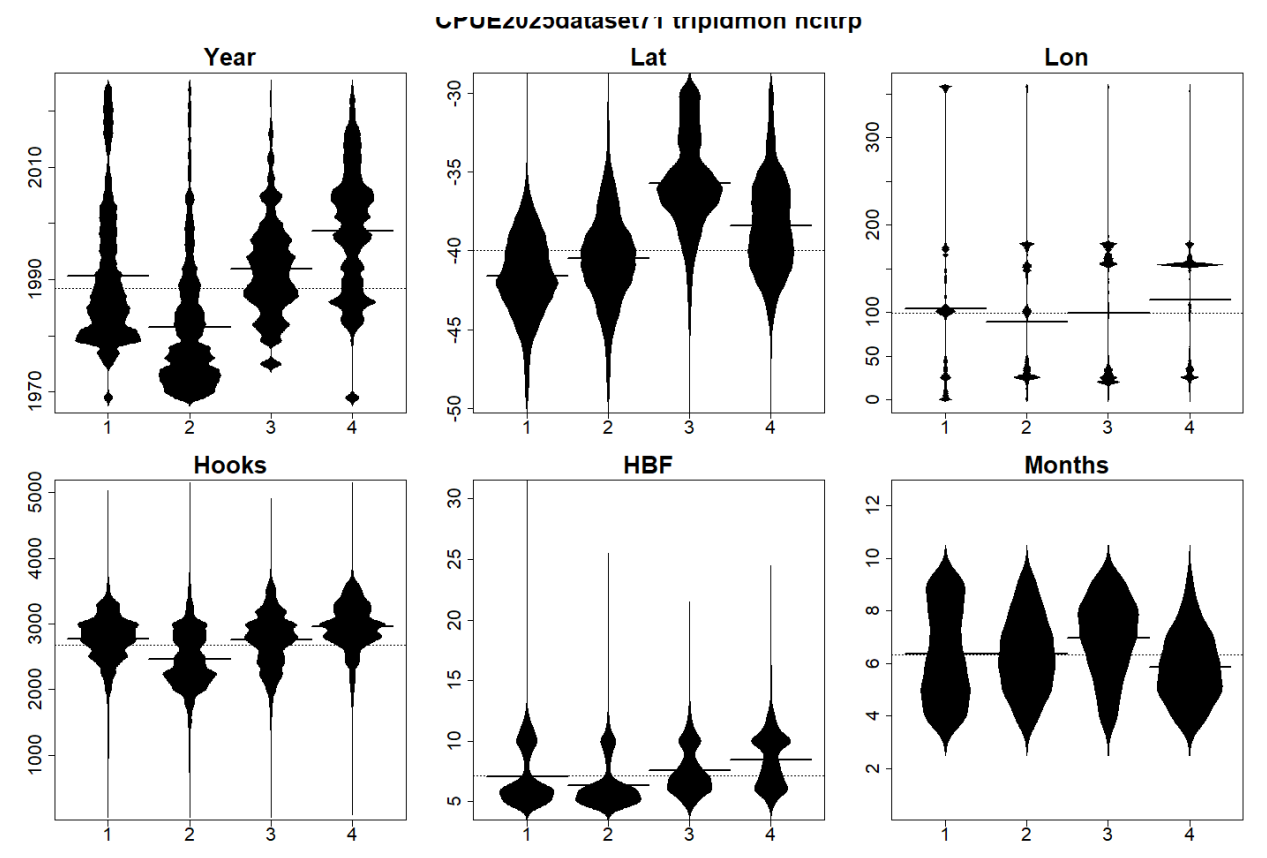


Fig. 7. Occurrence by variables of each group in the cluster analysis.

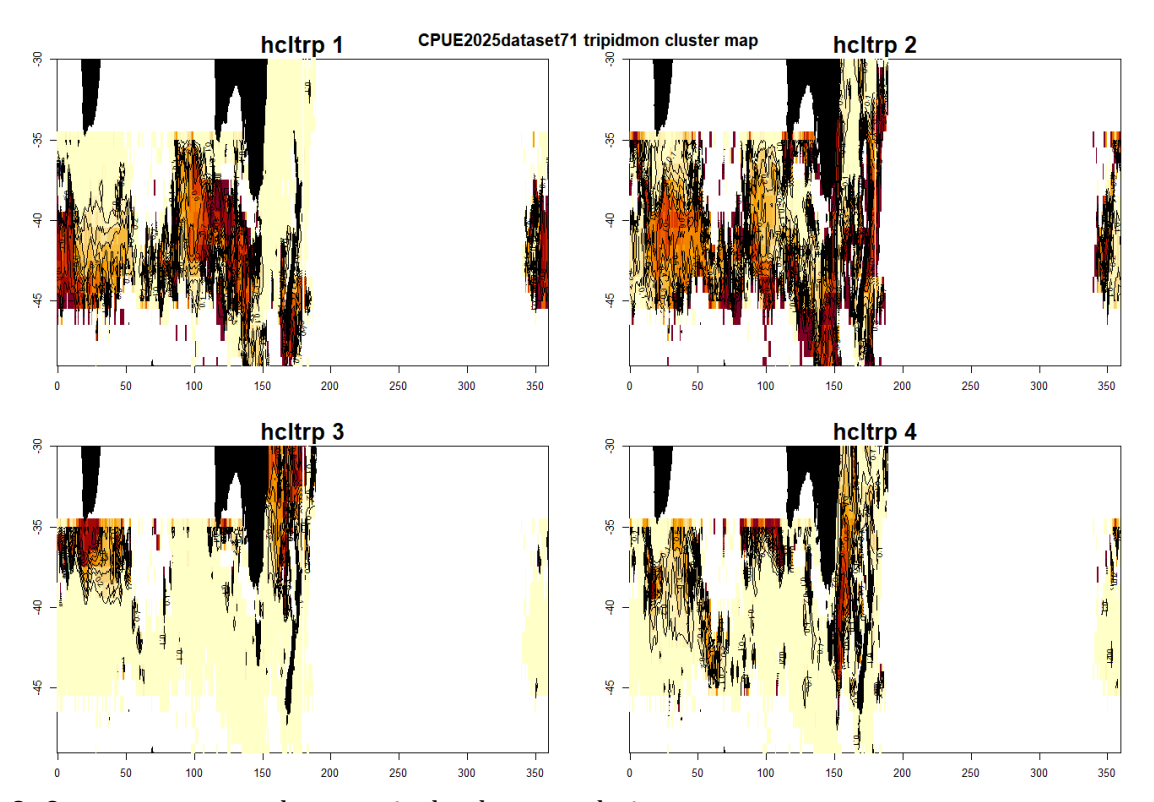


Fig. 8. Occurrence on map by group in the cluster analysis.

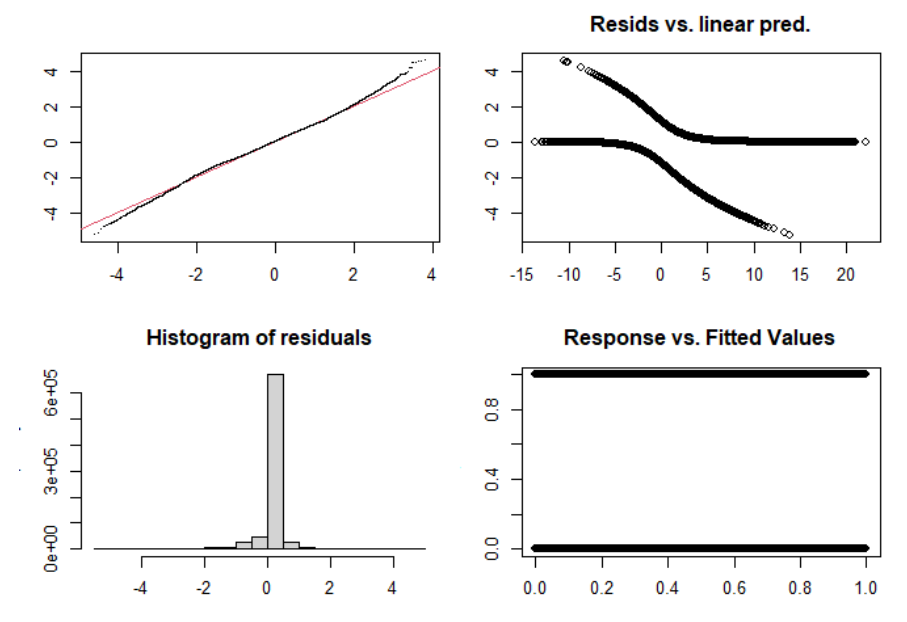


Fig. 9. Diagnostic plots for the binomial sub-model in the base case run.

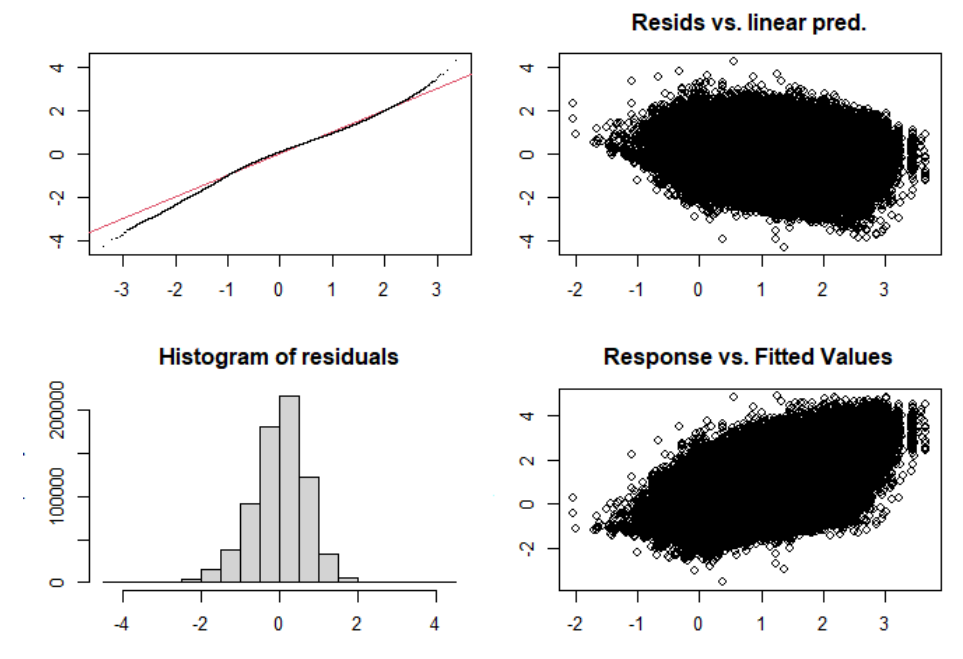


Fig. 10. Diagnostic plots for the positive catch sub-model in the base case run.

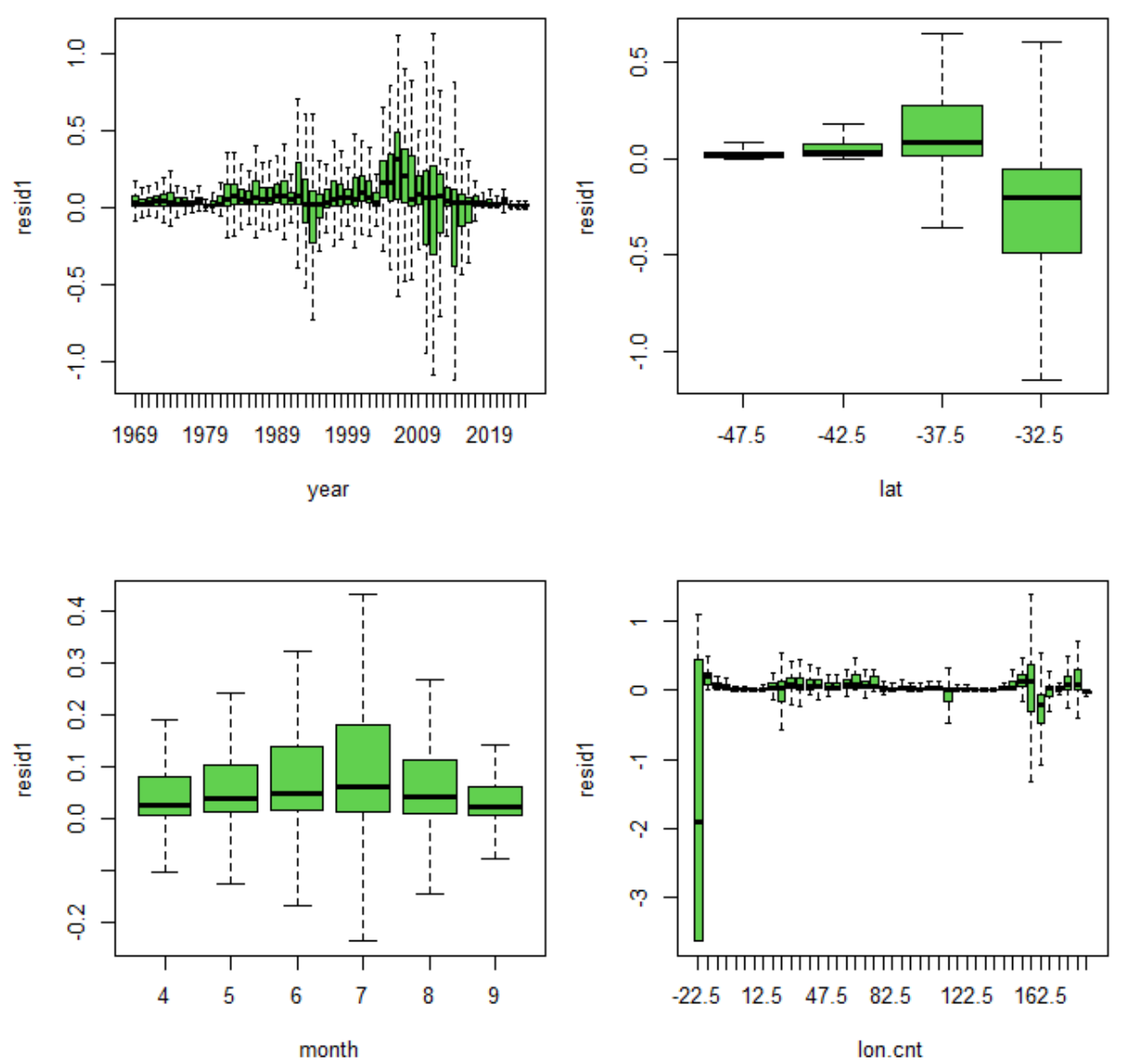


Fig. 11. Residuals by variable in the binomial sub-model in the base case run.

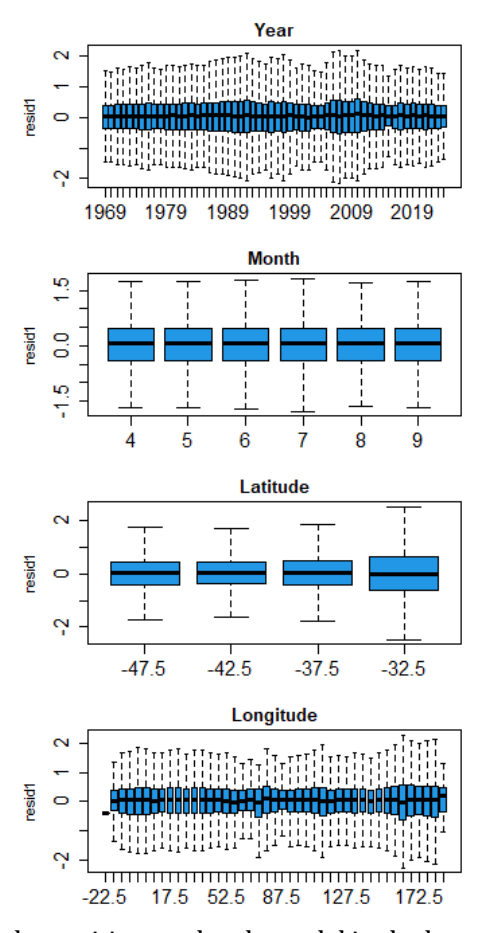


Fig. 12. Residuals by variable in the positive catch sub-model in the base case run.

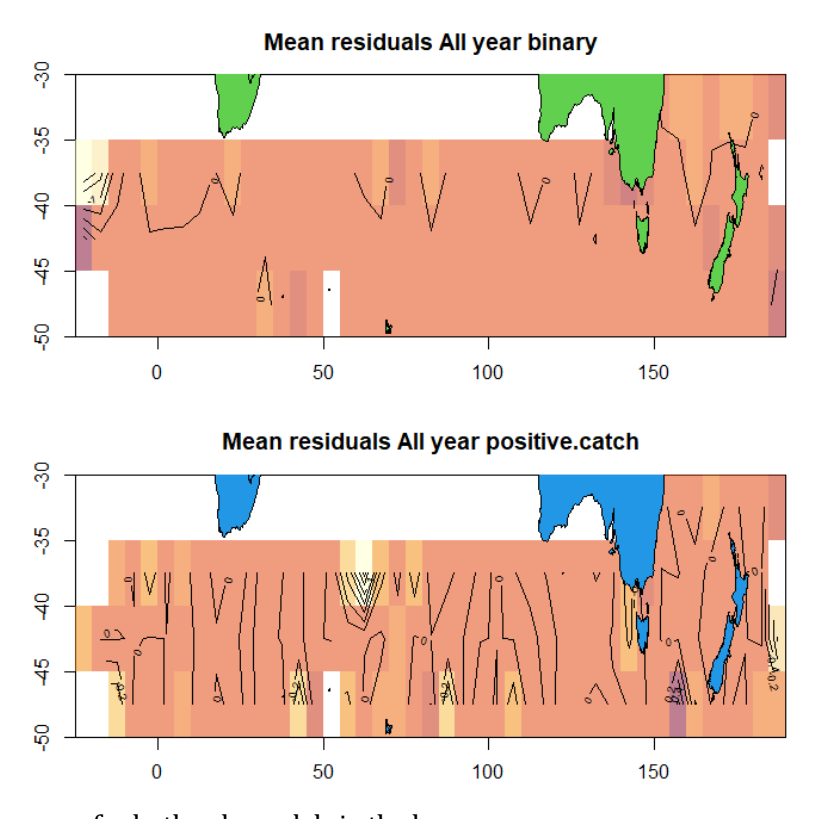


Fig. 13. Residual on maps for both sub-models in the base case run.

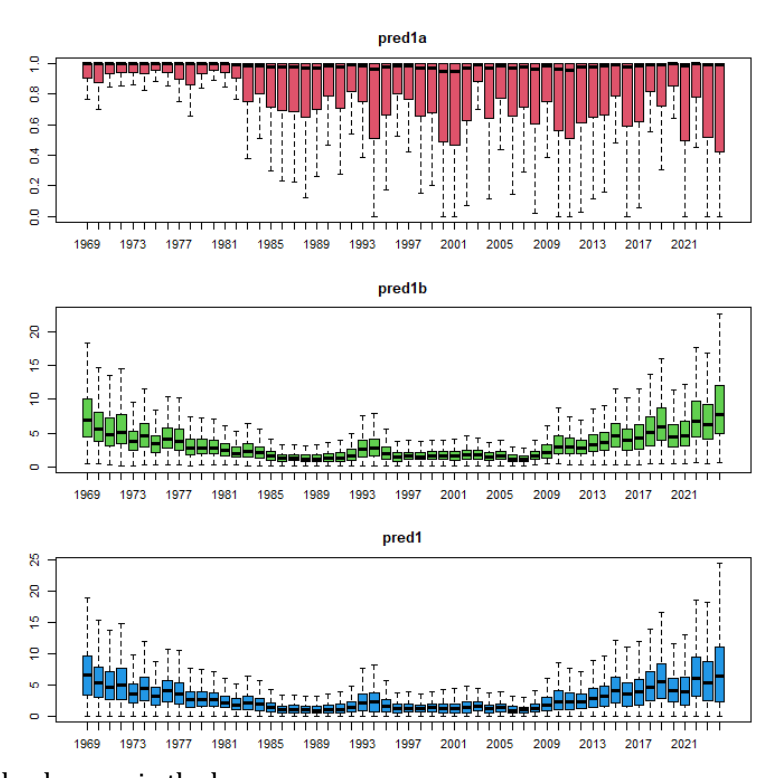


Fig. 14. Predicted value by year in the base case run.

Upper panel is the positive rate obtained from the binomial sub-model. Middle panel is CPUE obtained from the positive catch sub-model. Lower panel is the product of the two.

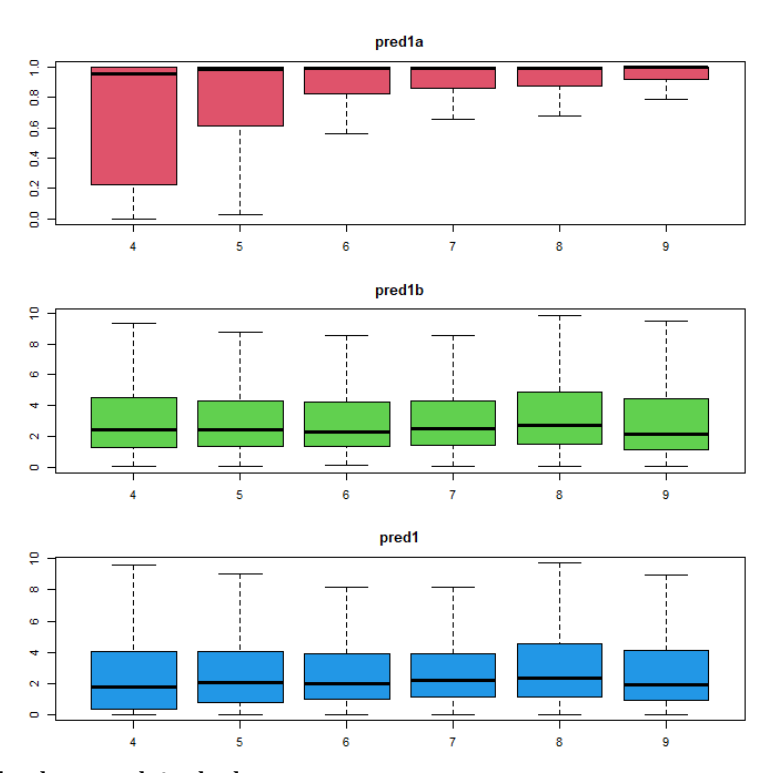


Fig. 15. Predicted value by month in the base case run. See Fig. 14.

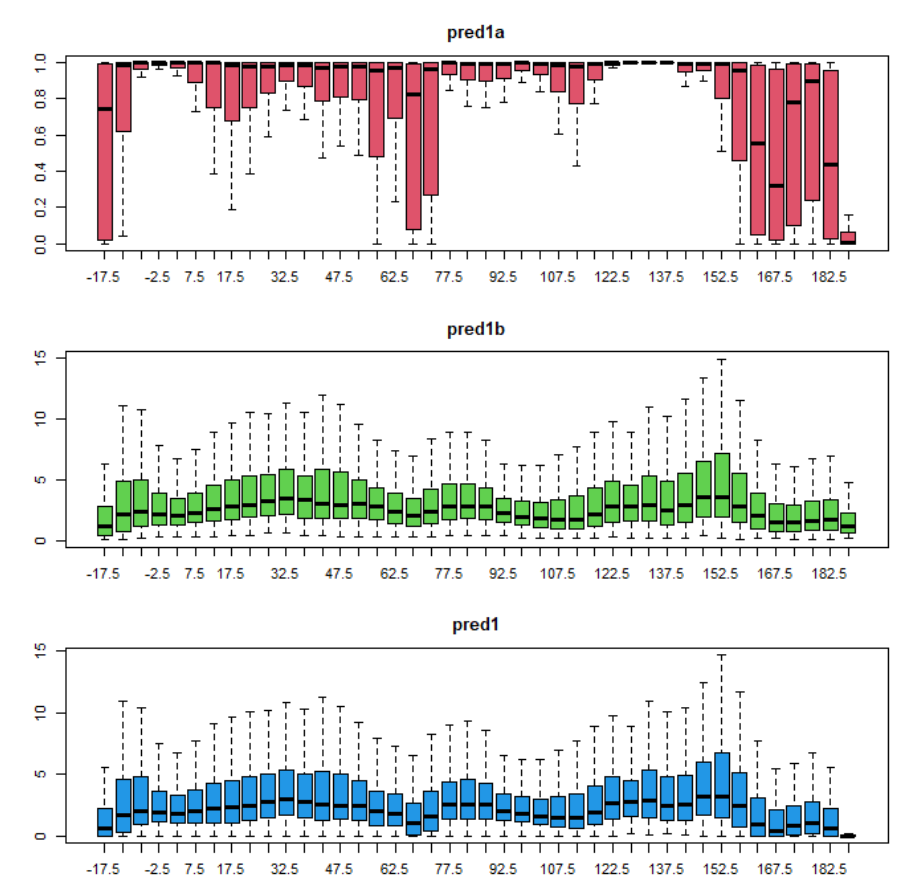


Fig. 16. Predicted value by longitude in the base case run. See Fig. 14. $\,$

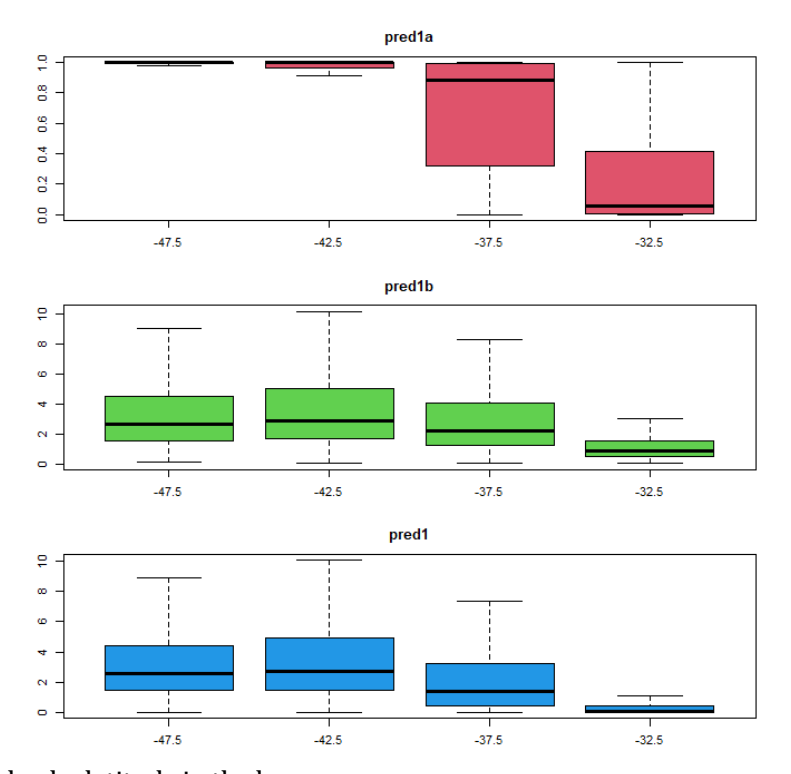


Fig. 17. Predicted value by latitude in the base case run. See Fig. 14.

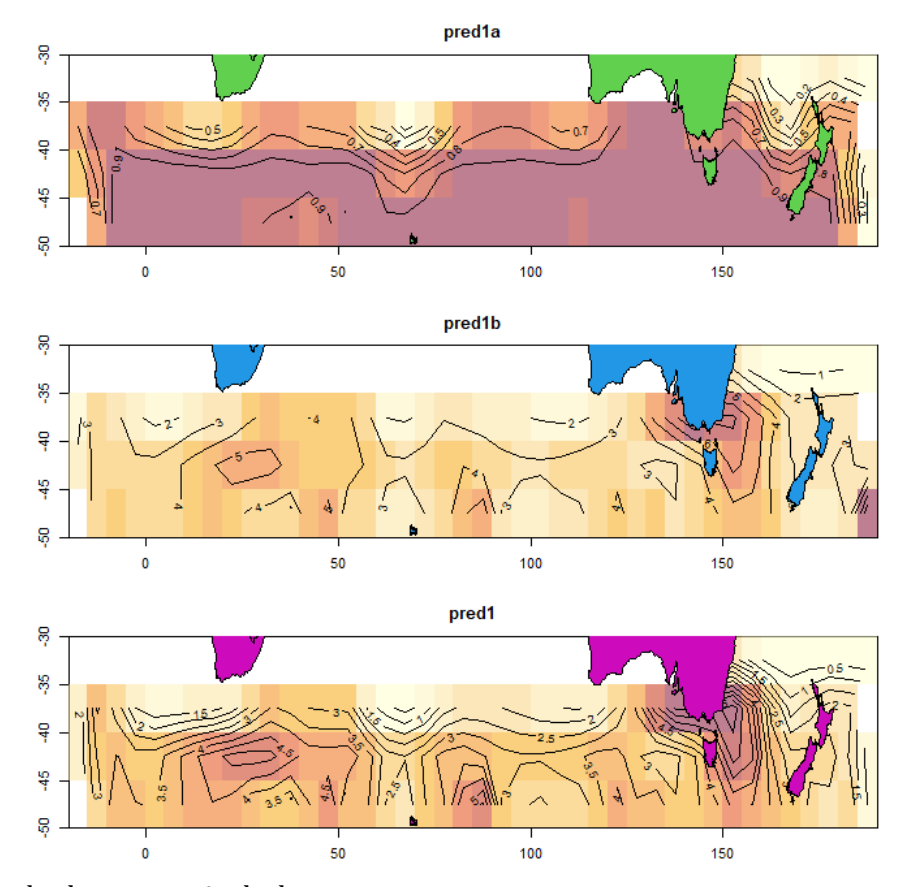


Fig. 18. Predicted value on map in the base case run. See Fig. 14.

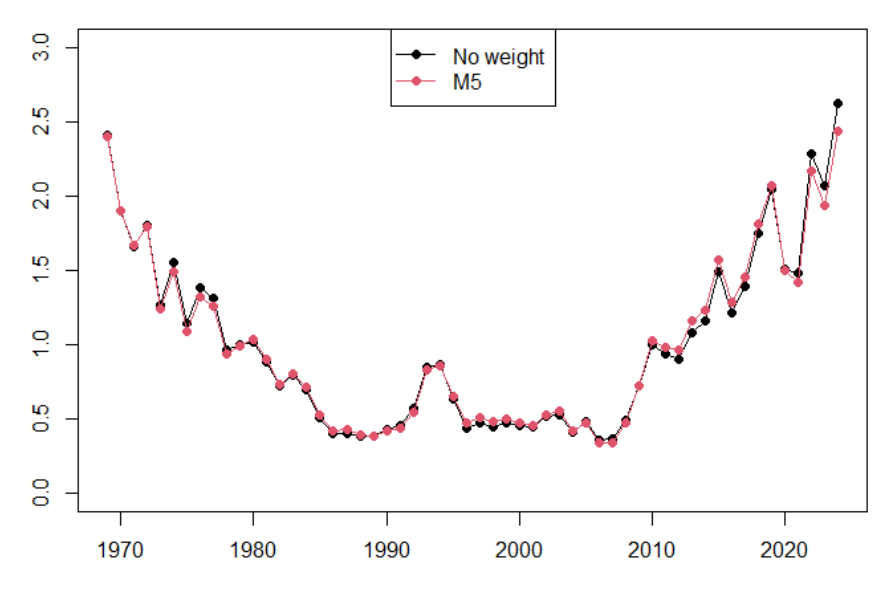


Fig. 19. Comparison of area weighted abundance indices in the base case run.

Red (M5) is area weighted abundance index of GAM22 which take into account that the longitude length changes over latitude and the number of 1x1 degree squares ever fished in a 5x5 degrees square. Black is the abundance index which weighting was not considered.

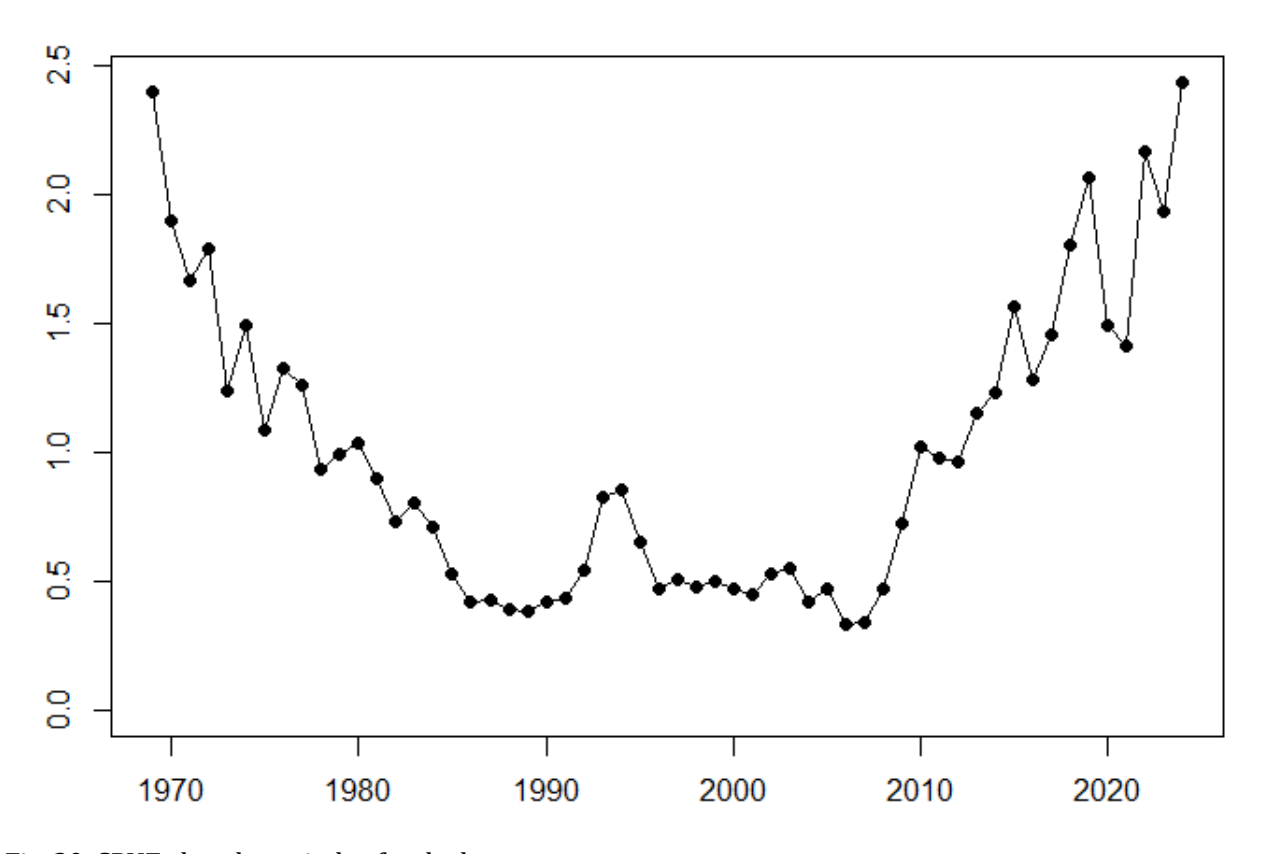


Fig. 20. CPUE abundance index for the base case.

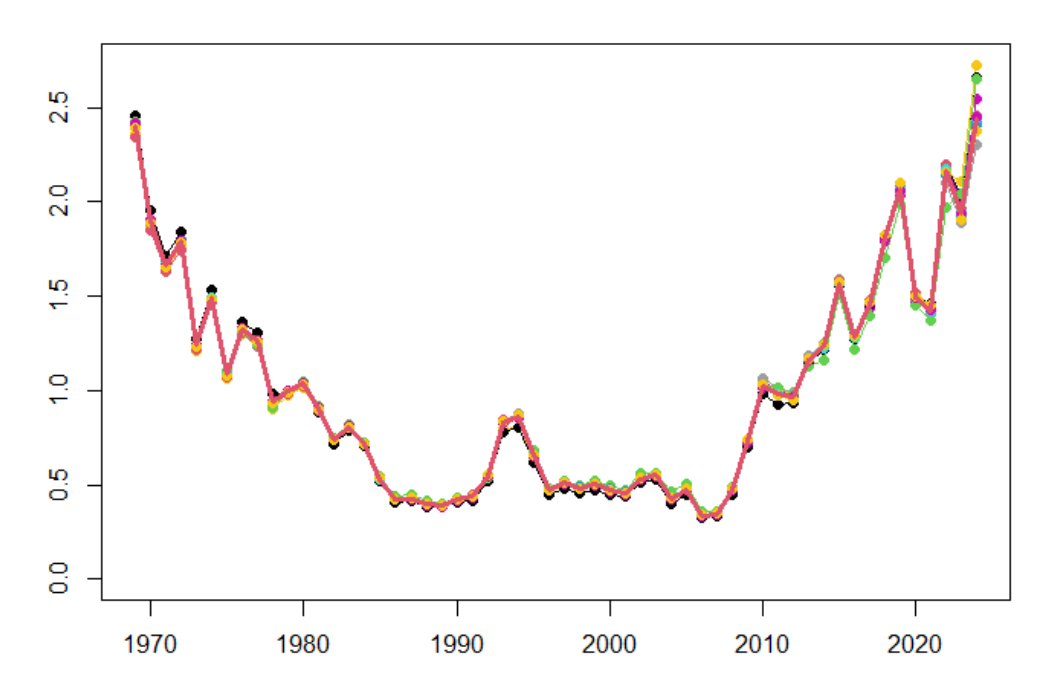


Fig. 21. Sensitivity analysis of model selection in the binomial sub-model for all runs.

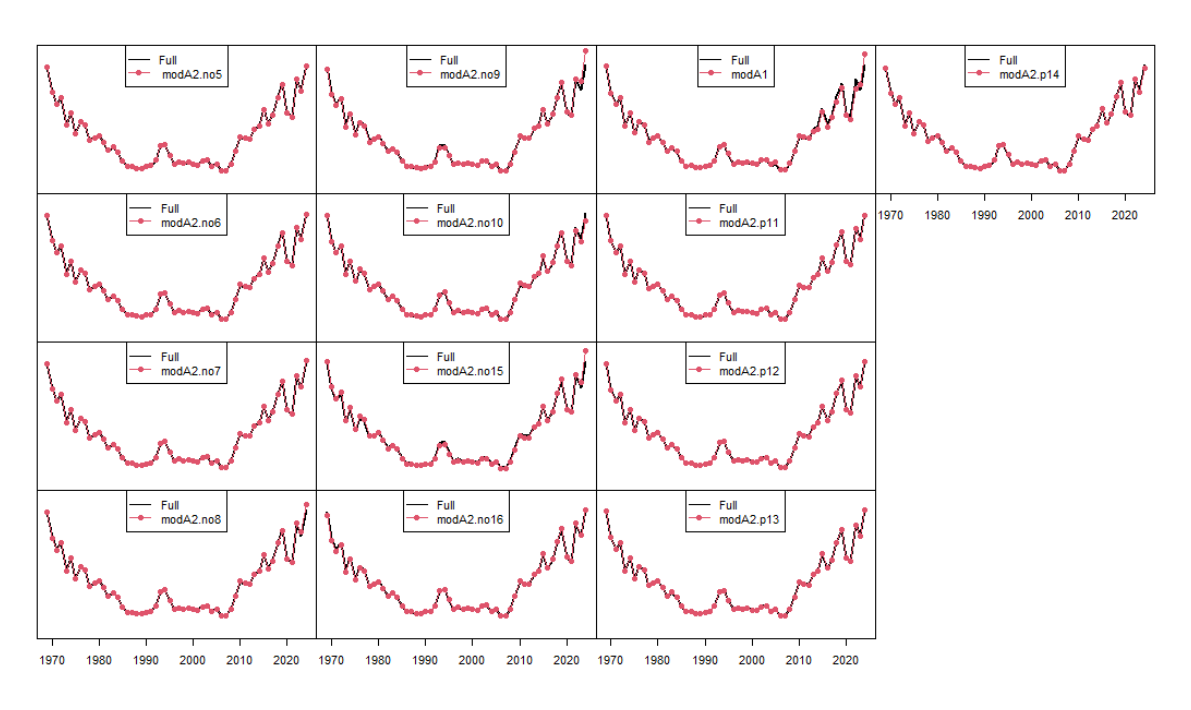


Fig. 22. Sensitivity analysis of model selection in the binomial sub-model for each run. Full represents ${\sf modA2}.$

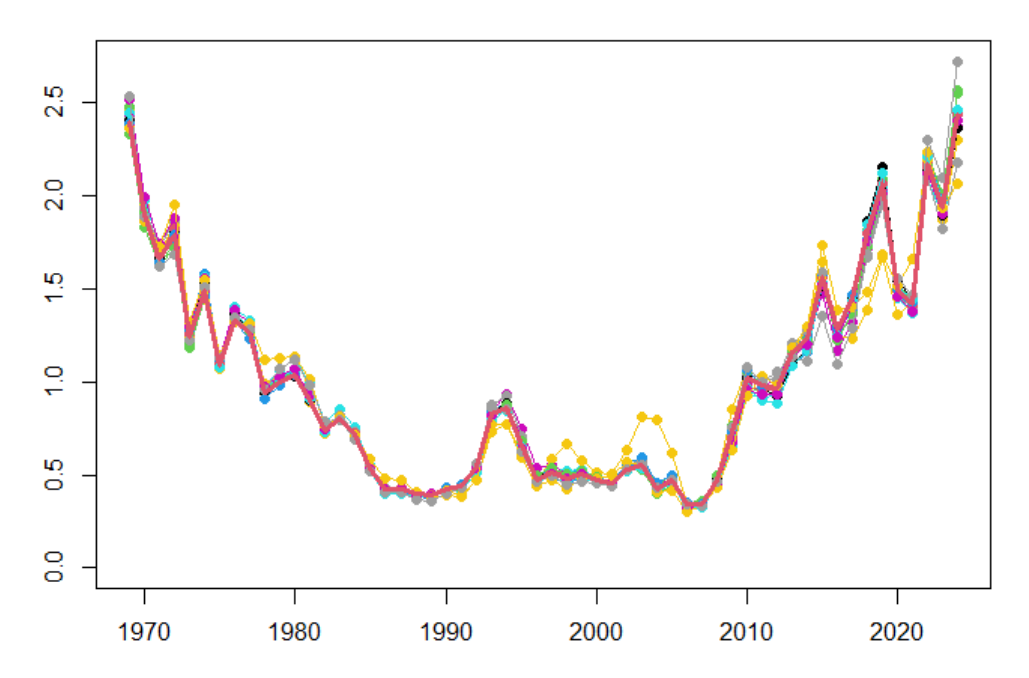
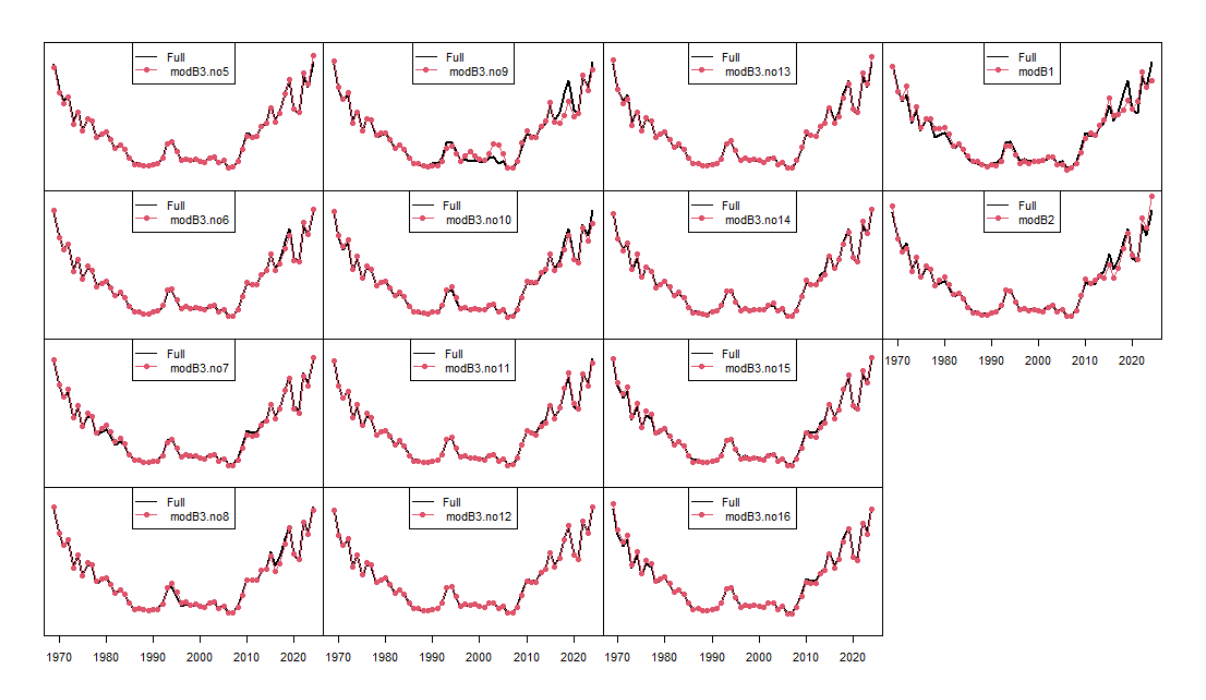


Fig. 23. Sensitivity analysis of model selection in the positive catch sub-model for all runs.



 $\label{eq:Fig. 24. Sensitivity analysis of model selection in the positive catch sub-model for each run. \\ Full represents mod B3.$

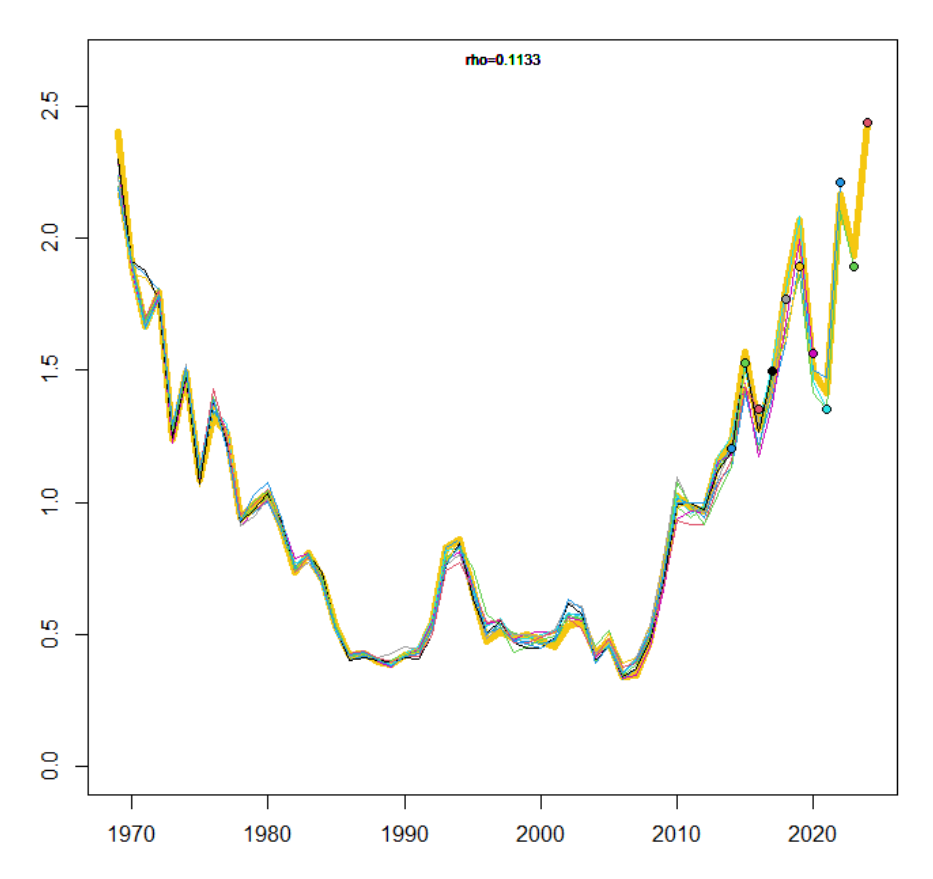


Fig. 25. Retrospective analysis for the base case model. Rho represents Mohn's rho.

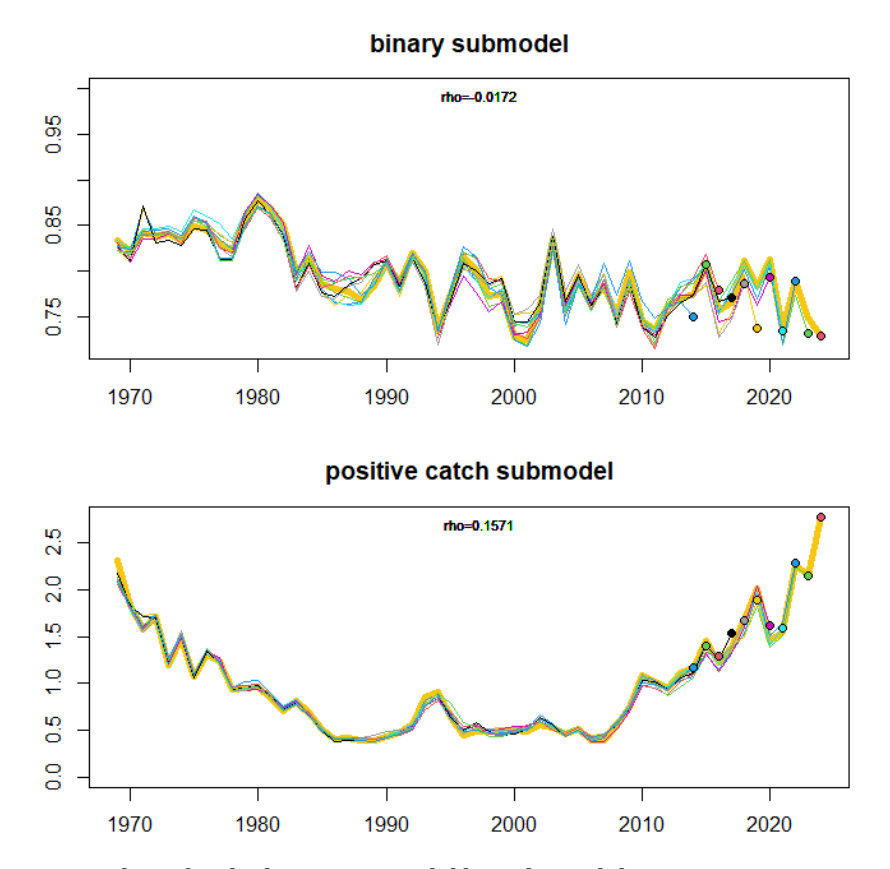


Fig. 26. Retrospective analysis for the base case model by sub-model.

Upper panel is by binomial submodel, and lower panel is by positive catch submodel. Rho represents Mohn's rho.

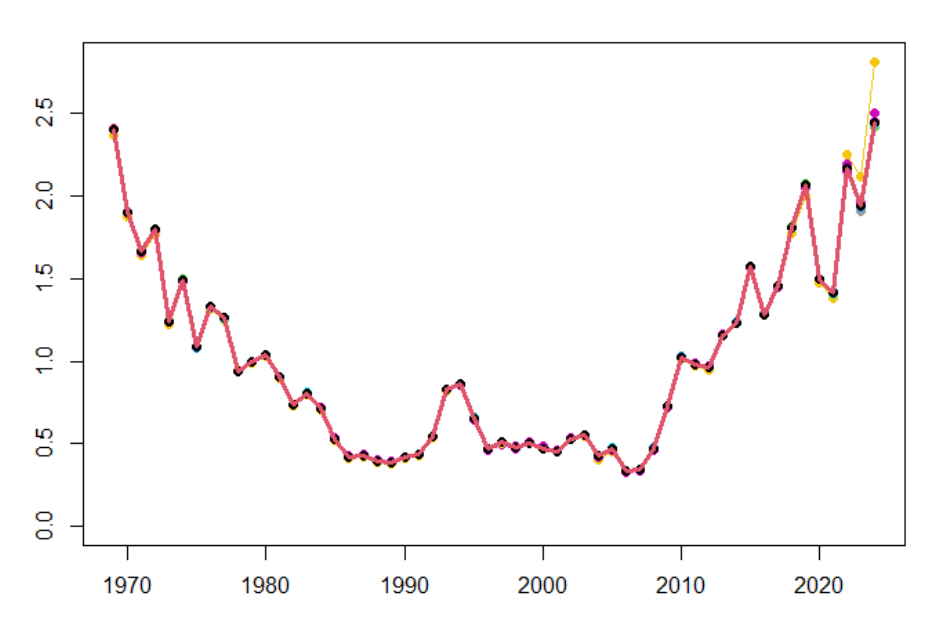


Fig. 27. Sensitivity analysis of k-value in the binomial sub-model for all runs.

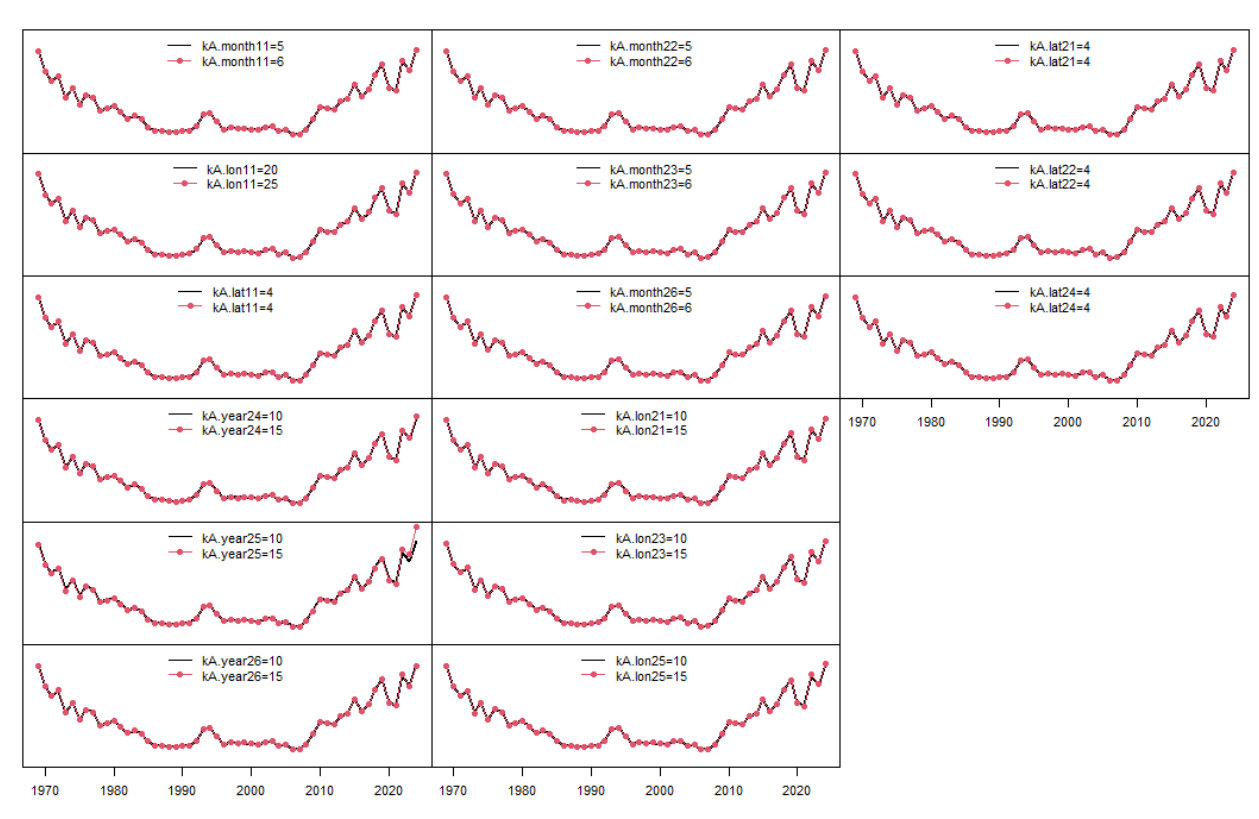


Fig. 28. Sensitivity analysis of k-value in the binomial sub-model for each of run.

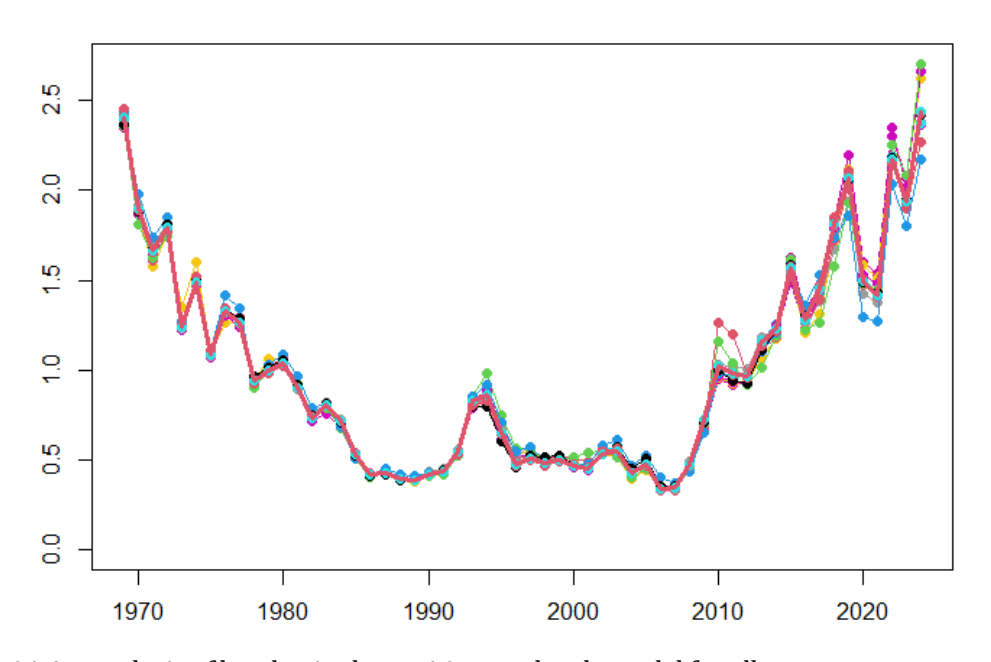


Fig. 29. Sensitivity analysis of k-value in the positive catch sub-model for all runs.

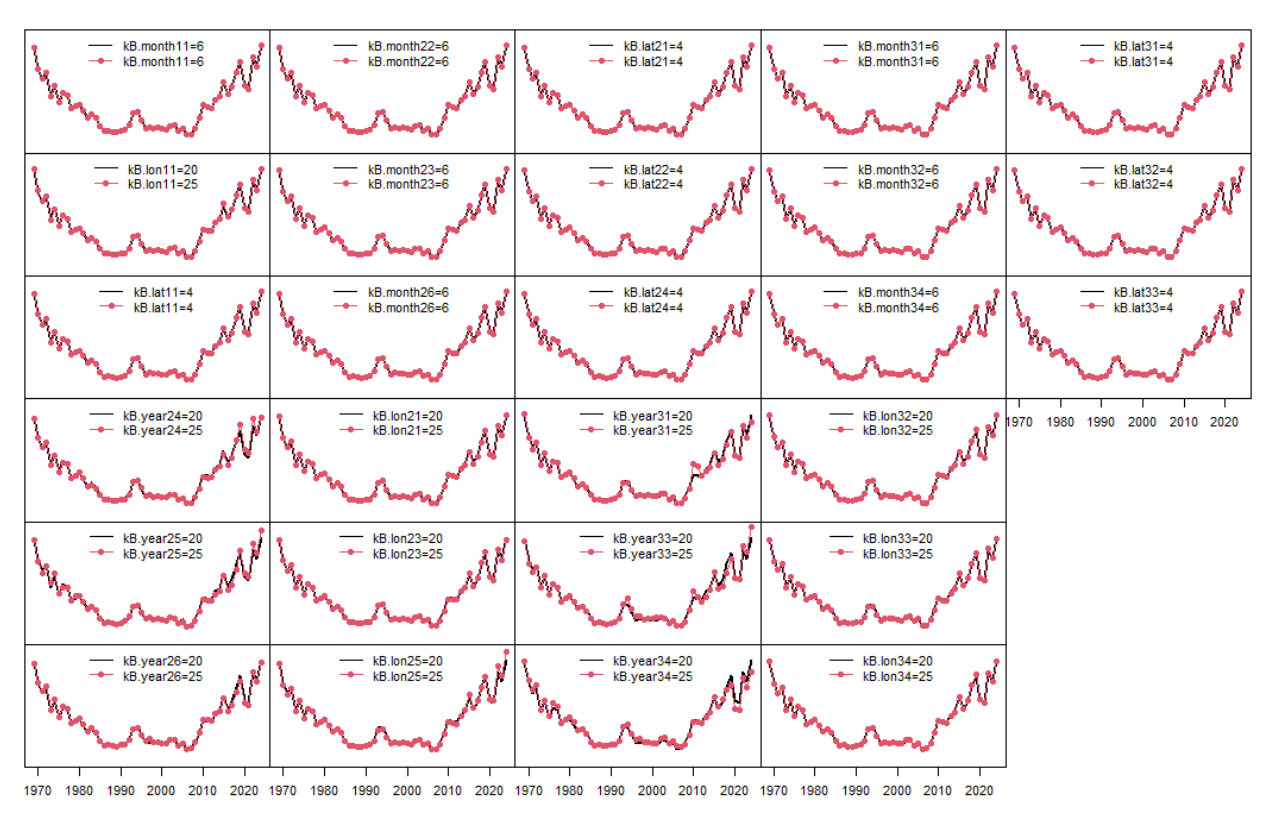


Fig. 30. Sensitivity analysis of k-value in the positive catch sub-model for each of run.

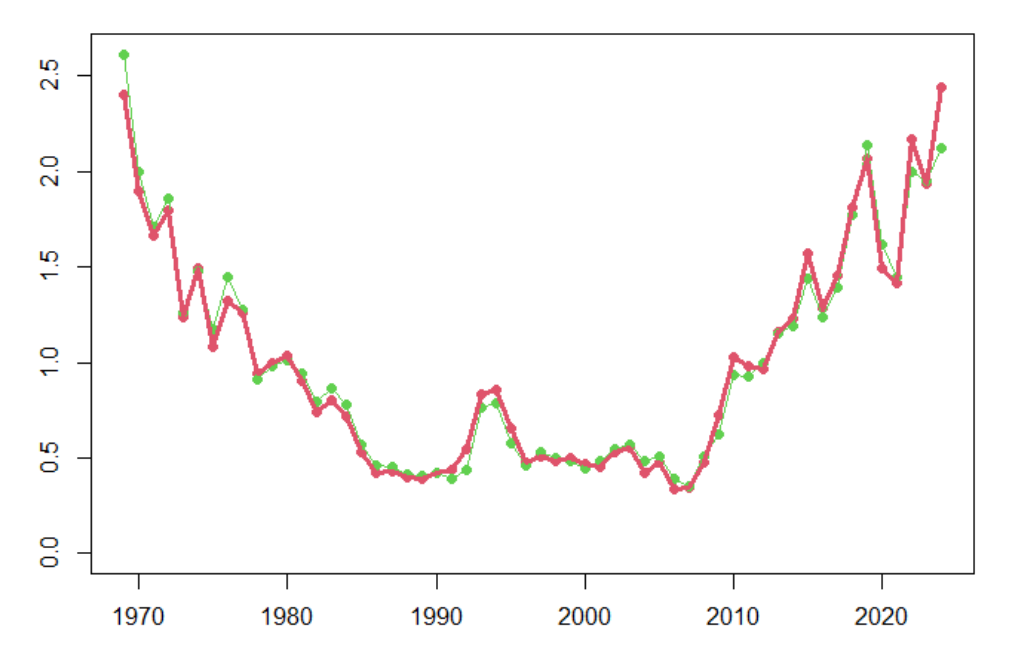


Fig. 31. Sensitivity analysis for the effect of age-5 plus instead of age-4 plus. Red is the base case, and green is the sensitivity run (age-5 plus).

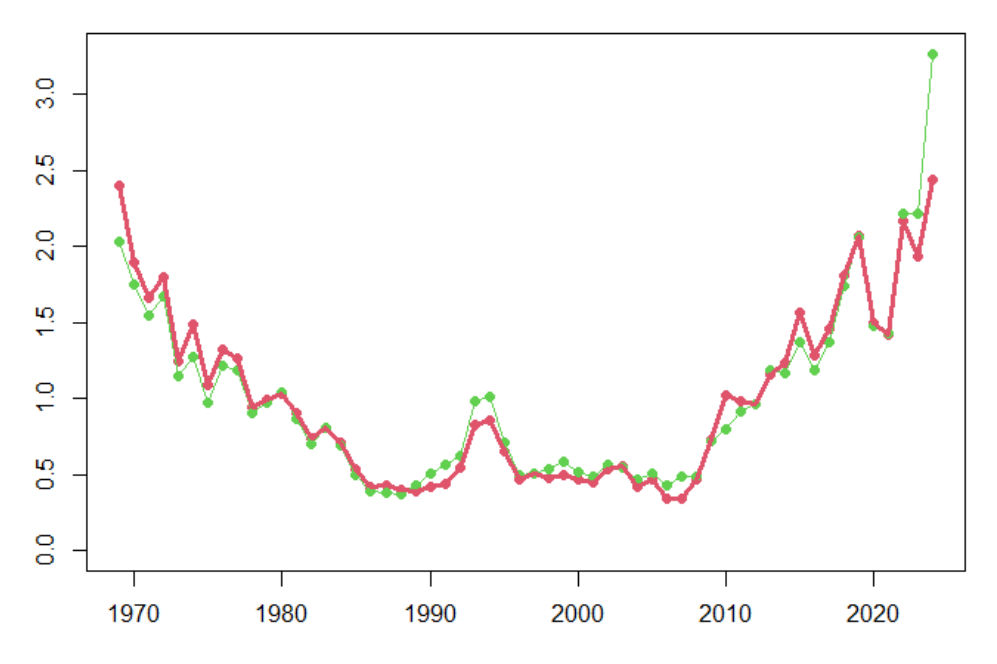


Fig. 32. Sensitivity analysis for the effect of of all ages instead of age-4 plus. Red is the base case, and green is the sensitivity run (all ages).

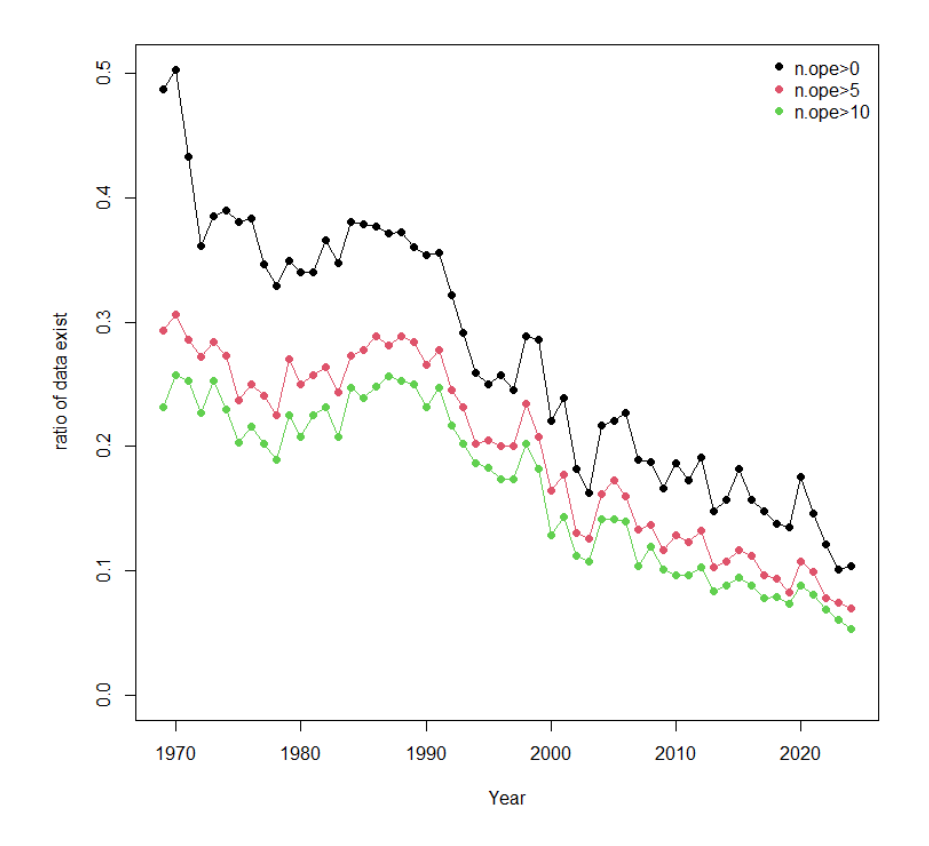


Fig. 33. Proportion of actual data existed in the dummy dataset used for glm/gam prediction by year. The numbers of operations >0, >5 and >10 are shown in black, red and green, respectively.

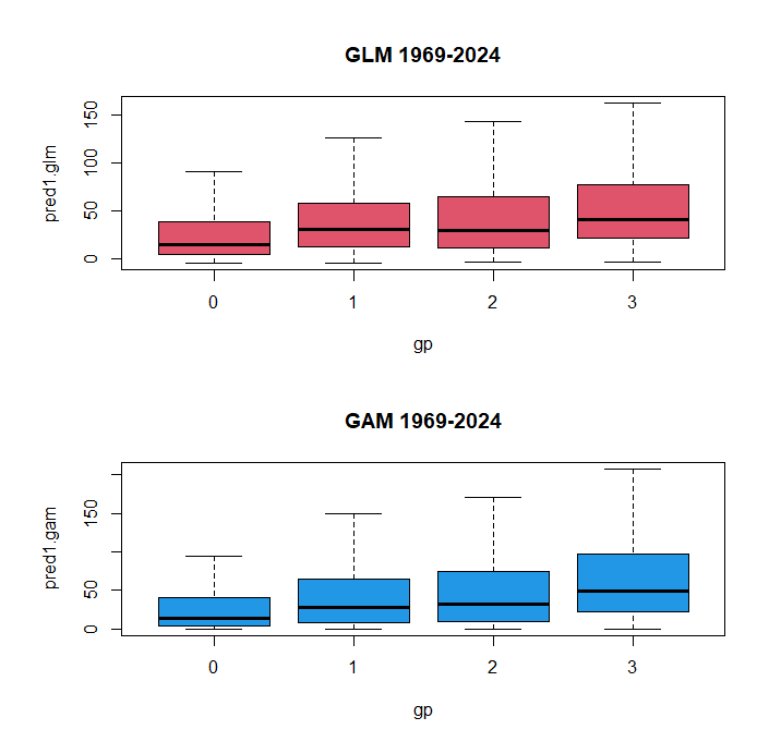


Fig. 34. Boxplot of CPUE predicted values by category group without outliers. Group 0 is the number of operations in actual data corresponded was 0. Group 1 is >=1 and <5 operations. Group 2 is >=5 and <10 operations and Group 3 is >10 operations. Data in all years were combined.

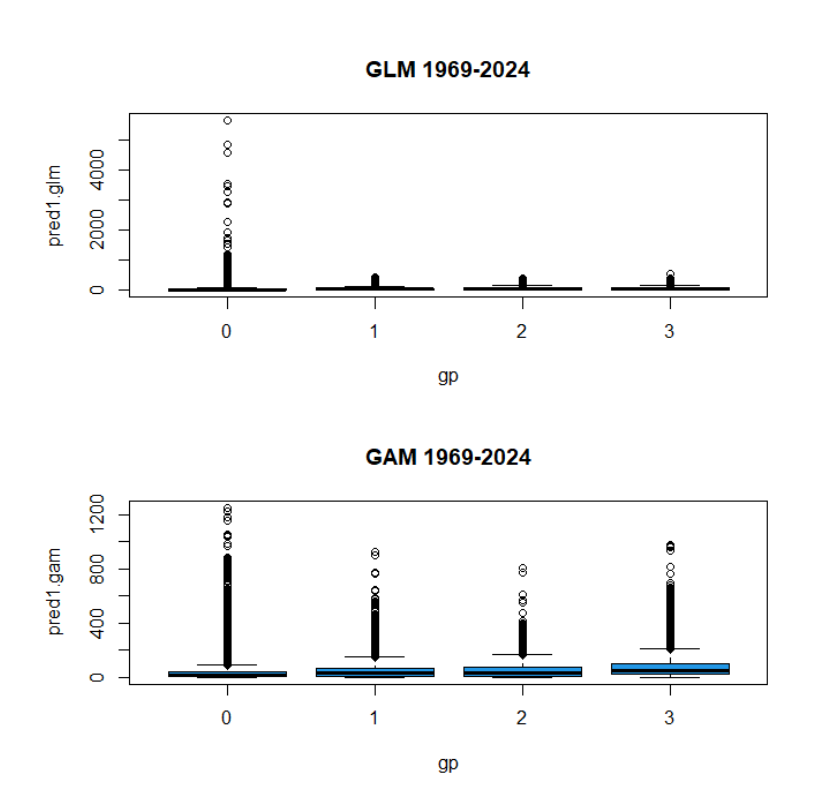


Fig. 35. Boxplot of CPUE predicted values by category group with outliers. Group 0 is the number of operations in actual data corresponded was 0. Group 1 is >=1 and < 5 operations. Group 2 is >=5 and < 10 operations and Group 3 is > 10 operations. Data in all years were combined.

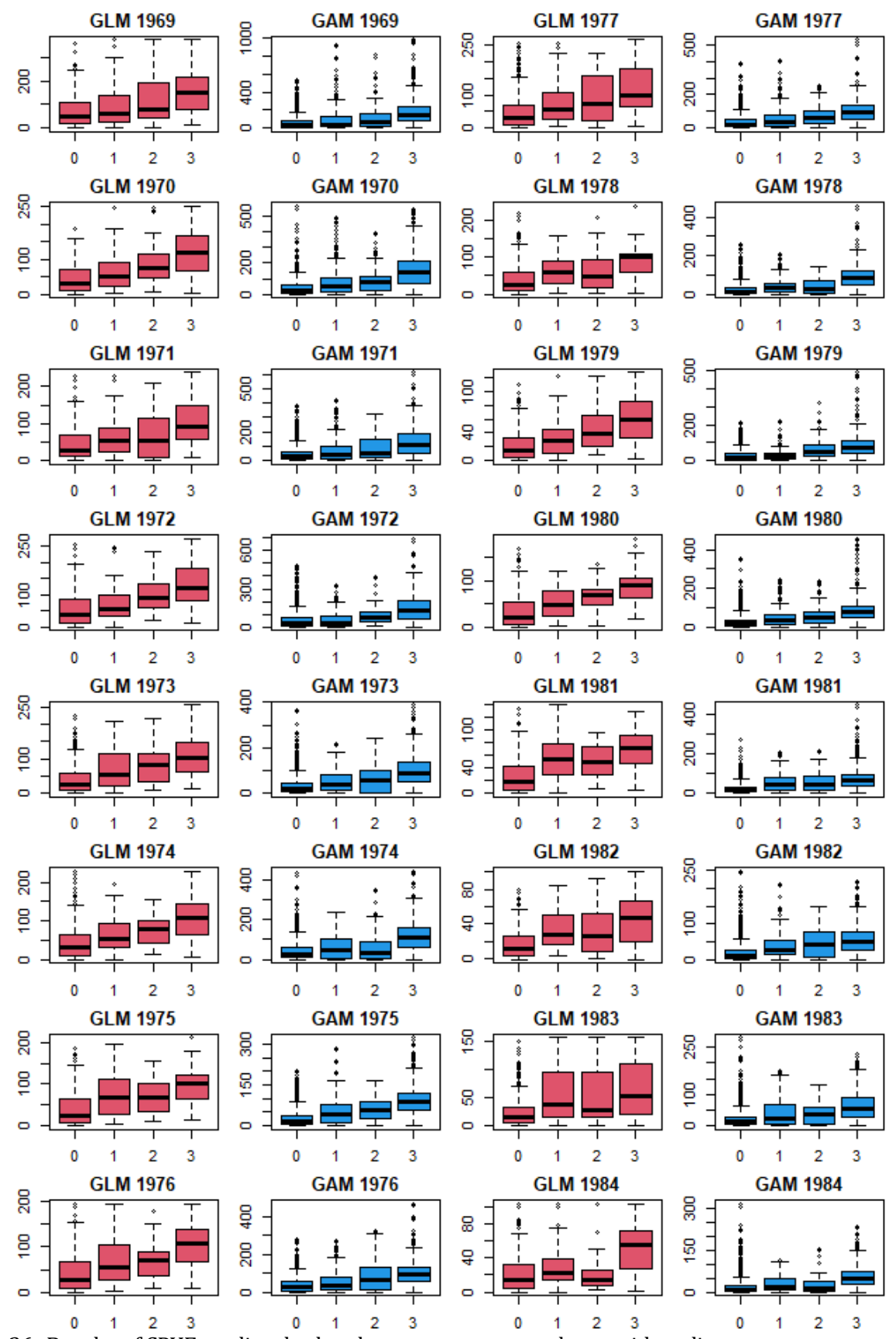
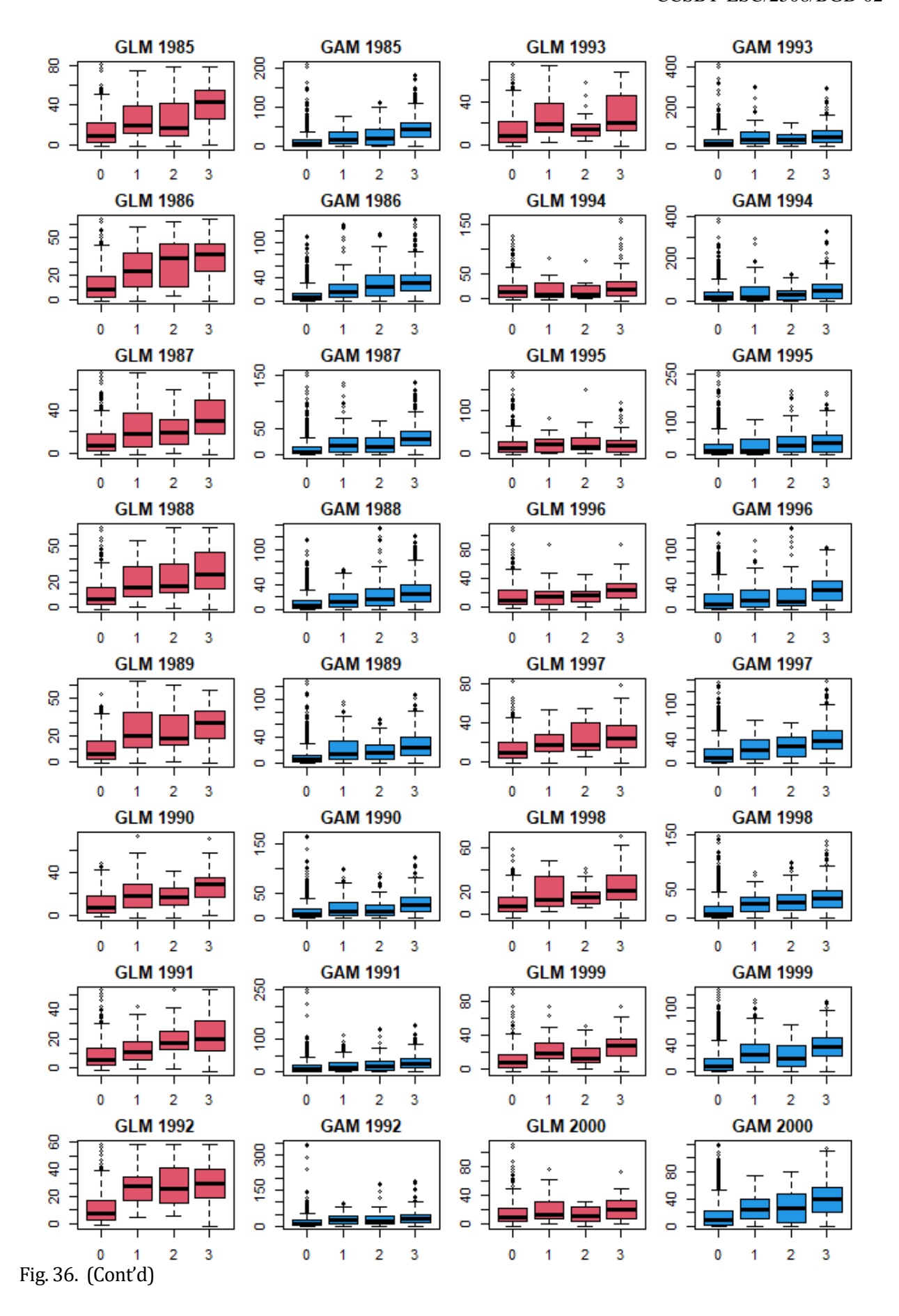
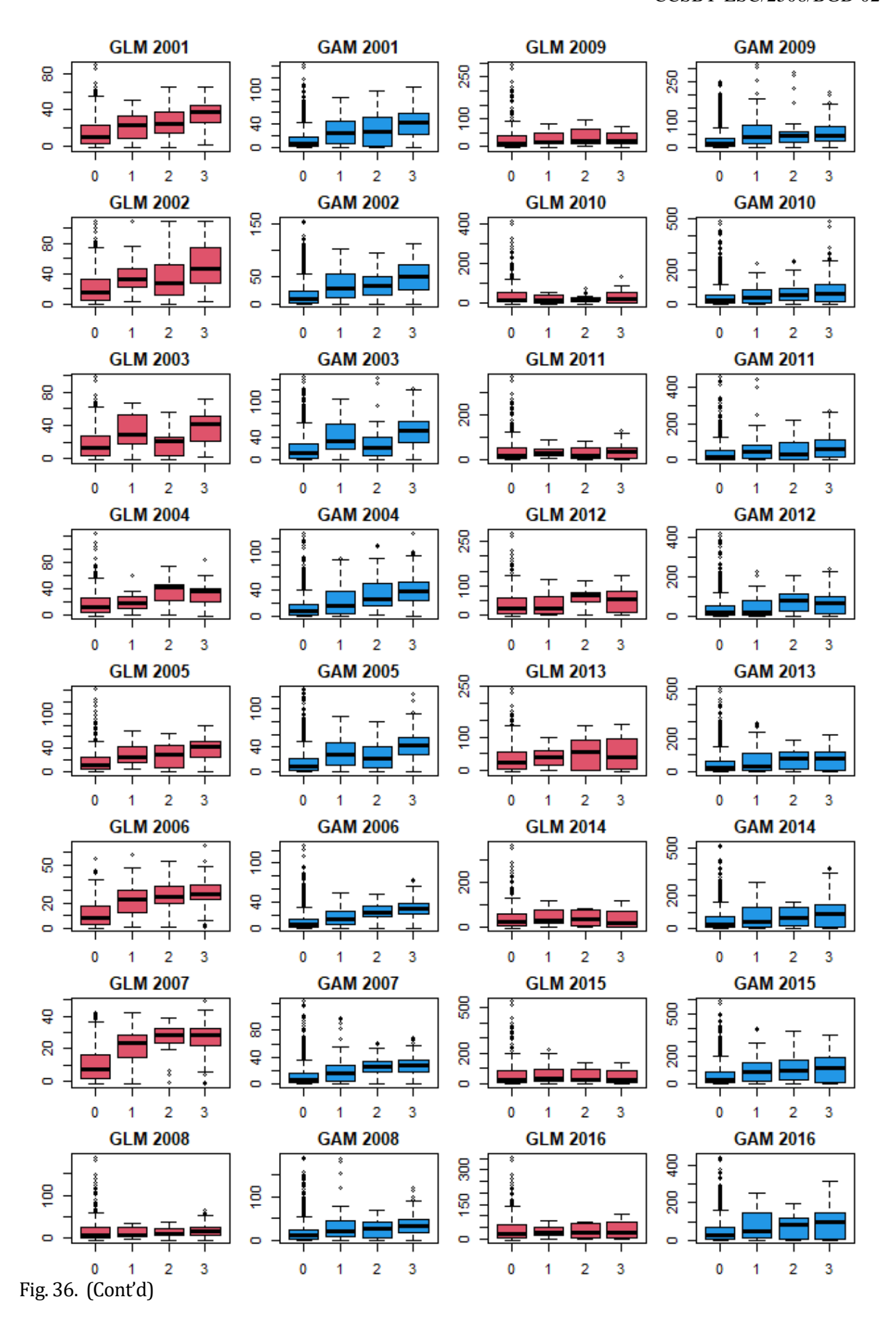
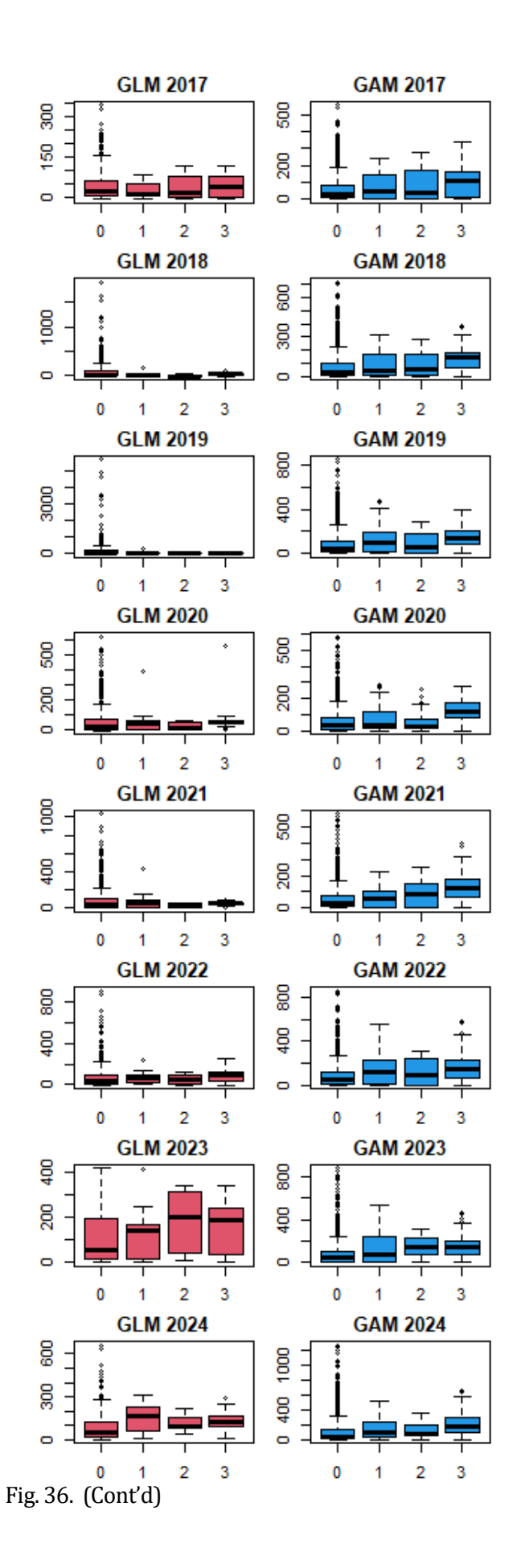


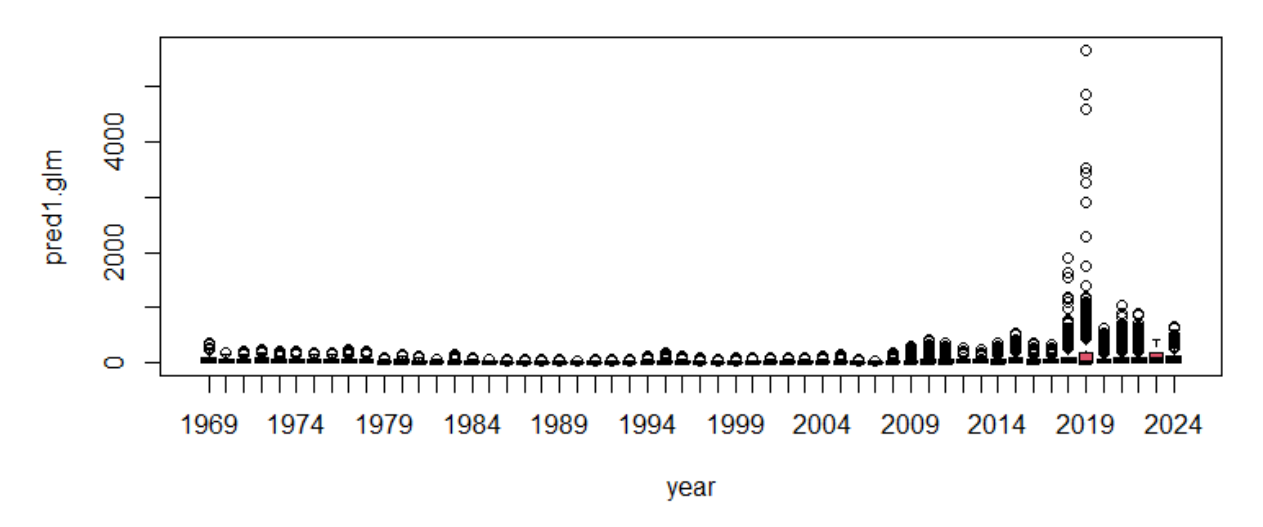
Fig. 36. Boxplot of CPUE predicted values by category group and year with outliers. Group 0 is the number of operations in actual data corresponded was 0. Group 1 is >=1 and <5 operations. Group 2 is >=5 and <10 operations and Group 3 is >10 operations.







GLM n.rec=0 by year



GAM n.rec=0 by year

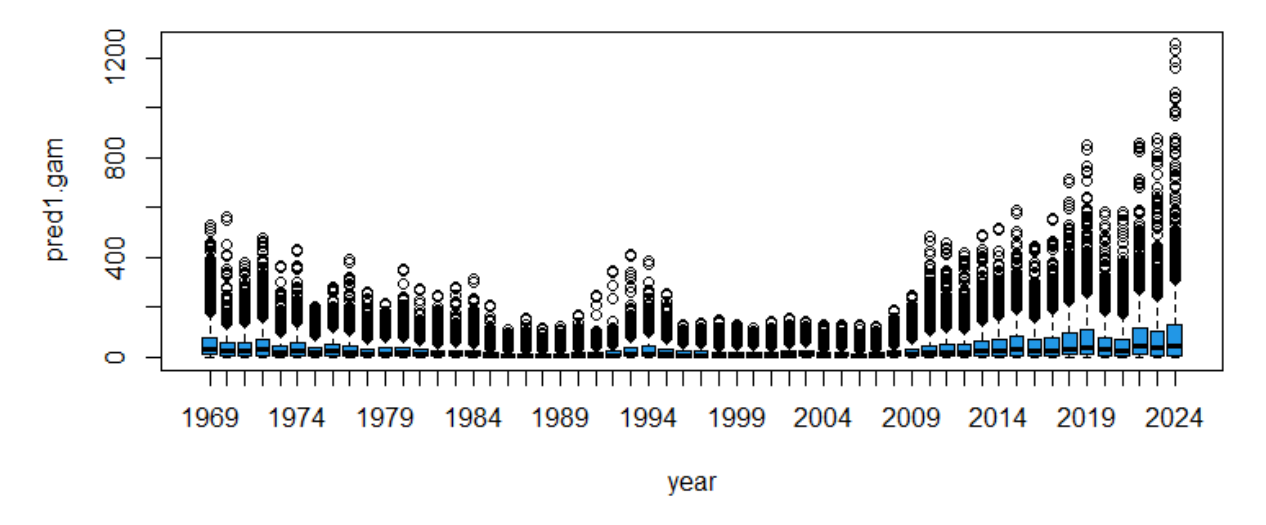


Fig. 37. Boxplot of CPUE predicted values by year in group 0, which no actual data corresponded.

Table 1. The k values selected for each of sub-model.

0.1.1.1	DOM	
Submodel	BSM	PCSM
k.month11	5	6
k.lon11	20	20
k.lat11	4	4
k.year24	10	20
k.year25	10	20
k.year26	10	20
k.month22	5	6
k.month23	5	6
k.month26	5	6
k.lon21	10	20
k.lon23	10	20
k.lon25	10	20
k.lat21	4	4
k.lat22	4	4
k.lat24	4	4
k.year31		20
k.year33		20
k.year34		20
k.month31		6
k.month32		6
k.month34		6
k.lon32		20
k.lon33		20
k.lon34		20
k.lat31		4
k.lat32		4
k.lat33		4

Table 2. Statistics of choosing \boldsymbol{k} values in the two sub-models of GAM.

Term	k'	edf	k-index	p-value
ti(month)	4	3.72	1.0135	0.93
ti(lon.cnt)	19	18.66	0.9866	0.31
ti(lat)	3	2.27	0.9841	0.26
ti(lon.cnt,lat)	27	18.28	0.9468	0.04
ti(month,lat)	12	8.53	0.9514	0.03
ti(lon.cnt,month)	36	31.22	0.9976	0.55
ti(year,lat)	27	22.45	0.9556	0.12
ti(year,lon.cnt)	81	72.93	0.8712	0.00
ti(year,month)	36	33.42	0.9772	0.27
s(log(hook))	9	8.33	0.9464	0.00

PCSM

Term	k'	edf	k-index	p-value
ti(month)	5	4.65	0.9938	0.31
ti(lon.cnt)	19	17.86	1.0112	0.79
ti(lat)	3	2.97	0.9735	0.03
ti(lon.cnt,lat)	42	33.44	1.0273	0.96
ti(month,lat)	14	10.93	0.9947	0.34
ti(lon.cnt,month)	94	72.12	1.0117	0.74
ti(year,lat)	57	44.68	1.0085	0.66
ti(year,lon.cnt)	333	248.29	0.9454	0.00
ti(year,month)	95	78.05	0.9823	0.10
ti(lat,month,year)	155	117.02	0.9751	0.07
ti(lat,lon.cnt,month)	90	69.20	1.0005	0.49
ti(lat,lon.cnt,year)	280	229.64	0.9579	0.01
ti(year,lon.cnt,month)	775	572.10	0.9526	0.00
s(log(hook))	9	7.65	0.9974	0.47

Table 3. Diagnostic statistics of GAM.

Sub-model	BSM	PCSM
n.data	803,697	710,827
dev.expl	73.78%	49.53%
AIC	151,419	1,508,124
residual.df	803,418	709,259
REMLscore	1,414,104	380,011

Table 4. Abundance index of GAM22 as the base case.

Year	Index		Year	Index
1969	2.40021		2001	0.45382
1970	1.89833		2002	0.53267
1971	1.66542		2003	0.55219
1972	1.79475		2004	0.42578
1973	1.24109		2005	0.47388
1974	1.49204		2006	0.33932
1975	1.08609		2007	0.34529
1976	1.32607		2008	0.47416
1977	1.26248		2009	0.72907
1978	0.94068		2010	1.02553
1979	0.99589		2011	0.98146
1980	1.03647		2012	0.96652
1981	0.90418		2013	1.15814
1982	0.73809		2014	1.23202
1983	0.80619		2015	1.56847
1984	0.71530		2016	1.28302
1985	0.53328		2017	1.45535
1986	0.42307		2018	1.80882
1987	0.42691		2019	2.06736
1988	0.39698		2020	1.49614
1989	0.38920		2021	1.41729
1990	0.42121		2022	2.16748
1991	0.43914		2023	1.93657
1992	0.54551		2024	2.43953
1993	0.83163			
1994	0.86105			
1995	0.65722			
1996	0.47323			
1997	0.51117			
1998	0.48278			
1999	0.50217			
2000	0.47228	-		

Table 5. Results of sensitivity analysis for model selection in the binomial sub-model.

name	term	dev.expl	AIC	residual.df	REMLscore	dAIC
modA2	Main and 2 way interactions	73.78%	151,419	803,418	1,414,104	2,646
modA2.no5	-ti(lon, lat)	73.35%	153,900	803,436	3,629,272	5,127
modA2.no6	-ti(month, lat)	73.53%	152,855	803,426	3,468,809	4,082
modA2.no7	-ti(lon, month)	73.49%	153,068	803,449	1,584,605	4,295
modA2.no8	-ti(year, lat)	73.07%	155,492	803,437	2,719,582	6,719
modA2.no9	-ti(year, lon)	72.53%	158,498	803,491	1,197,277	9,725
modA2.no10	-ti(year, month)	72.92%	156,330	803,450	1,181,875	7,557
modA2.no15	-cl	70.97%	167,613	803,417	2,217,587	18,840
modA2.no16	-s(log(hook))	73.38%	153,708	803,426	1,426,858	4,935
modA1	Main effects	67.66%	186,274	803,604	1,256,535	37,501
modA2.p11	+ti(lat, month, year)	74.16%	149,287	803,394	7,696,093	514
modA2.p12	+ti(lat, lon, month)	74.05%	149,940	803,390	335,983,501	1,167
modA2.p13	+ti(lat, lon, year)	74.02%	150,120	803,390	2,422,050	1,347
modA2.p14	+ti(year, lon, month)	74.26%	148,773	803,368	1,081,397	0

Table 6. Results of sensitivity analysis for model selection in the positive catch sub-model.

name	term	dev.expl	AIC	residual.df	REMLscore	dAIC
modB3	Full model	49.53%	1,508,124	709,259	380,011	0
modB3.no5	-ti(lon, lat)	49.51%	1,508,483	709,243	380,173	360
modB3.no6	-ti(month, lat)	49.50%	1,508,623	709,254	380,158	499
modB3.no7	-ti(lon, month)	49.46%	1,509,251	709,229	380,446	1,127
modB3.no8	-ti(year, lat)	49.53%	1,508,154	709,249	380,061	30
modB3.no9	-ti(year, lon)	49.37%	1,510,516	709,226	380,735	2,392
modB3.no10	-ti(year, month)	49.51%	1,508,374	709,262	380,084	250
modB3.no11	-ti(lat, month, year)	49.48%	1,508,671	709,321	380,071	547
modB3.no12	-ti(lat, lon, month)	49.47%	1,508,900	709,277	380,203	776
modB3.no13	-ti(lat, lon, year)	49.21%	1,512,293	709,416	380,826	4,170
modB3.no14	-ti(year, lon, month)	48.52%	1,521,131	709,789	382,492	13,007
modB3.no15	-cl	49.14%	1,513,606	709,256	381,393	5,482
modB3.no16	-s(log(hook))	49.50%	1,508,634	709,261	380,139	510
modB1	Main effects	41.53%	1,609,783	710,733	402,802	101,659
modB2	Main and 2 way interactions	47.48%	1,534,536	710,194	385,174	26,412

Table 7. Summary statistics of the estimates where CPUE predicted value > 1500, in group 0 in the GLM model.

Year	Area	Month	Ν	Mean	Max	Sum
2018	8	6	4	1,555	1,555	6,218
2018	8	7	4	1,646	1,646	6,583
2018	8	8	4	1,913	1,913	7,654
2019	8	6	20	2,883	4,598	57,669
2019	8	7	12	3,805	4,866	45,655
2019	8	8	12	4,213	5,657	50,550
2019	8	9	8	1,754	1,754	14,030

Table 8. Summary statistics of the estimates where CPUE predicted value > 800, in group 0 in GAM22.

Year	Area	Month	N	Mean	Max	Sum
2019	4	9	2	840	849	1,681
2022	4	8	2	836	845	1,673
2022	4	9	2	850	858	1,699
2023	4	8	2	811	820	1,623
2023	4	9	2	869	878	1,738
2024	4	7	2	850	859	1,700
2024	4	8	3	992	1,059	2,976
2024	4	9	4	1,098	1,254	4,391
2024	7	4	7	988	1,183	6,915